Expression and regulatory mechanisms of SNAP25 and Syntaxin 1A in H9c2 cells

Dan Gheorghiu

A THESIS SUBMITTED TO
THE FACULTY OF GRADUATE STUDIES
IN PARTIAL FULFILLMENT OF THE REQUIREMENTS
FOR THE DEGREE OF
MASTER OF SCIENCE

GRADUATE PROGRAM IN BIOLOGY
YORK UNIVERSITY
TORONTO, ONTARIO

October 2019

Abstract

Two SNARE proteins, SNAP25 and STX1A, are widely expressed in neurons and neuroendocrine cells, and more recently, shown to be expressed in the heart, but their underlying mechanisms remain unknown. This study examined the regulation of SNAP25 and STX1A gene promoters in the cardiac cell line, H9c2. The cells were treated with the HDAC inhibitor, trichostatin A (TSA), forskolin to activate PKA, or retinoic acid to induce differentiation to a more cardiac phenotype. The data showed greater activity of the -292 bp SNAP25 promoter compared to the -1517 bp full-length construct. Similarly, the -204 bp promoter constructs of STX1A were higher than the full-length -1931 bp promoter. Neither treatment with TSA, forskolin nor retinoic acid induced expression of SNAP25 or STX1A in H9c2 cells. The results demonstrate SNARE protein expression cannot be induced in H9c2 cells. Further studies are required to determine the regulation of SNARE proteins in the heart.

Keywords: promoter activity, HDAC inhibition, PKA activation, differentiation

Acknowledgements

The scope of this project and writing of this thesis would not have been possible without the tutelage of my supervisor, Dr. Tsushima. He gave me an opportunity I could otherwise not have gotten anywhere else, and his constant support, humor and guidance has made this entire process most enjoyable. I would also like to thank my committee member, Dr. John McDermott, for his invaluable feedback throughout this project.

I cannot thank my lab mate, Manvir Virdi, enough for all the time he spent teaching me all the techniques, apparatus, and procedures of the lab. His continued patience through two years of questions and brainstorming made this project much more streamlined. On the same line, I would like to also thank Xiaodong Gao for always making herself available to help and going above and beyond in helping me troubleshoot lab issues.

I would like to thank my partner, Holly Echlin, for helping me handle the stress and worries that come with a master's thesis. She has been an emotional foundation for me throughout my master's degree, and my gratitude for her is immeasurable. Finally, I would like to thank my family for their continued support throughout all of this, and especially my father for having helped shape the man I want to become; may he rest in peace.

Table of Contents

Abstract ii
Acknowledgements iii
Table of Contents iv
List of Tables v
List of Figures vi
Introduction 1
Mammalian Heart and its Endocrine Functions 1
SNARE Proteins 2
Syntaxin 1A 8
SNAP25 9
Transcriptional Mechanisms 10
Epigenetic Regulation of Cells 14
Trichostatin A 15
Forskolin 18
Retinoic Acid 20
INS-1 832/13 Cell Line 23
H9c2 Cell Line 24
Purpose and Hypotheses 29
Materials and Methods 32
Cell Culturing 32
Cell Passaging 32
HDAC Inhibitor Treatment 33
PKA Activation Treatment 34
Cell Differentiation 34
Cell Lysis and Preparation 35
Bradford Assay 35
Western Blotting 35
Bacterial Transformation of STX1A and SNAP25 38
Plasmid Purification, Isolation, and Quantitation 40
RNA Isolation and Quantitation 42
RNA to cDNA Conversion and Polymerase Chain Reaction 43
Cell Transfection 46
Luciferase Assay and Promoter Activity 47
Statistical Analysis 48
Results 50
Luciferase Reporter Activity 50
Western Blotting Analysis 58
PCR and DNA electrophoresis 64
Discussion 65
Luciferase Analysis 66
Protein Expression and Densitometry 69
Conclusions 71
References 72

List of Tables

Table 1: Primary and secondary antibodies 37

Table 2: DNA primer forward and reverse sequences 45

List of Figures

Figure 1: SNARE mediated exocytosis 7

Figure 2: Simplified diagram showcasing TFs at work 13

Figure 3: Histone acetylation and deacetylation 17

Figure 4: Diagram showcasing cyclic AMP activation 19

Figure 5: Retinoic acid binds to retinoic acid receptors 22

Figure 6: H9c2 cells in their undifferentiated state 27

Figure 7: H9c2 cells that have been differentiated by RA 28

Figure 8: pGL3 Vector into which truncated regions were inserted 39

Figure 9: SNAP25 promoter activity in INS-1 832/13 cells 54

Figure 10: STX1A promoter activity in INS-1 832/13 cells 55

Figure 11: SNAP25 promoter activity in H9c2 cells 56

Figure 12: STX1A promoter activity in H9c2 cells 57

Figure 13: Western blotting of SNARE proteins 60

Figure 14: Densitometry analysis on cTnT blots 61

Figure 15: Densitometry analysis on MyoG blots 62

Figure 16: Western blotting of SNARE proteins with Sp1 63

Introduction

Mammalian Heart and its Endocrine Functions

As a highly evolved and complex closed 'ecosystem', the human body's organs can communicate with each other seamlessly and effortlessly. While other organs contain some form of redundancy, the heart is a sophisticated muscular organ that is integral to the survival of many animals. At its most basic level, the heart consists of four chambers, two chambers called 'atria', and another two chambers called 'ventricles' located inferior to the atria (Gomez Stallons et al., 2016). As a part of the autonomic nervous system, the heart is at the center of the circulatory system, as all the blood gets pumped to every part of the body and its extremities, and blood also gets carried back to the heart for re-oxygenation via the lungs (Florea & Cohn, 2014). This back and forth flow of blood and its constituents is controlled by the various valves in the heart, with the mitral and tricuspid valve controlling the flow of blood from atria to ventricles, and the aortic and pulmonary valve controlling the flow of blood out of the ventricles. These valves ensure that blood flows in the right direction and backflow does not occur. (Gomez Stallons et al., 2016). This action of pumping is performed via electrical signals and carried out by the musculature of the heart, known as myocardium; hence the medical term for a heart attack being myocardial infarction (Steg et al., 2012).

Long having been thought that the heart functions solely as a muscle for pumping blood, it has also been found to function as an endocrine organ (de Bold, Borenstein, Veress, & Sonnenberg, 1981; Peters, Miller, & Giovannucci, 2006). Mammalian heart atria have been shown to secrete the peptide hormones atrial natriuretic peptide (ANP) and brain natriuretic peptide (BNP) to help maintain extracellular fluid volume and blood pressure, respectively (Sagnella, 2002). ANP was discovered in 1981 when rat atrial muscle extracts were shown to

increase salt output in the kidney (De Bold, 1985). ANP is first released when distention of the heart tissue occurs, and when released by atrial myocytes, it functions by binding to natriuretic peptide receptor A (NPRA) as an agonist, in turn increasing renal sodium excretion, resulting in a decrease of extracellular fluid volume.

BNP, although secreted by ventricular myocytes instead, is similar in function to ANP. It also acts on NPRA receptors as an agonist, however with twice the half-life of ANP, making it a better blood diagnostic tool. Agonist binding to NPRA receptors causes a reduction in sodium reabsorption in the kidneys, resulting in increased blood volume. However, it also has the secondary effect of improving blood ejection fraction, therefore causing a reduction in blood pressure (Cauliez, Berthe, & Lavoinne, 2005). As with any hormones and neurotransmitters, the mediation of ANP and BNP is regulated via a family of proteins known as SNAREs.

SNARE Proteins

The role of soluble *N*-ethylmaleimide-sensitive factor attachment protein receptor (SNARE) proteins have long been studied since the 1980s and established in the mediation of membrane-fusion and exocytotic release of neurotransmitters in the brain for the better part of the last few decades (Han, Pluhackova, & Böckmann, 2017). SNARE proteins are a large protein superfamily, originally found in yeast and identified to play a role as receptors, key components of synaptic membranes, and as components required for the fusion of membranes and secretion of proteins (Burri & Lithgow, 2004).

SNARE proteins in mammals were first discovered in the brain via mutations on two proteins: N-ethylmaleimide sensitive factor (NSF) and soluble NSF-attachment protein (SNAP; Glick and Rothman 1987). The mutations of NSF and SNAP allowed for the discovery of their

binding constituents, syntaxin and synaptosomal-associated protein of 25 kDa (SNAP25). This allowed for more profound research and the discovery of SNARE proteins' role in the process of exocytosis in neuronal and neuroendocrine cells (e.g. pituitary and hypothalamus). Within the last decade, research on SNARE proteins and their role in the heart has been steadily increasing, helping to elucidate how the heart may act as an endocrine organ as well (de Bold et al., 1981; Peters et al., 2006), with the likes of the mammalian heart atria having been shown to secrete the hormones ANP and BNP to help maintain extracellular fluid volume and blood pressure, respectively. Peters and colleagues (2006) showed a thorough SNARE expression profile via western blotting and found that adult rat cardiac myocytes do indeed express SNARE proteins (e.g. SNAP25, SNAP23, STX4, etc.), but there is no expression of these proteins in neonatal rat cardiac myocytes. The importance of SNARE proteins in the heart was further highlighted by Ferlito and colleagues (Ferlito et al., 2010) when their team was able to show that by introducing small interfering RNA (siRNA), levels of ANP secretion decreased. The siRNA sequence they introduced was designed to knockdown levels of syntaxin 4 in rat cardiac myocytes, such that even with the addition of endothelin-1 (a vasoconstrictor), ANP was being released in reduced amounts, at higher doses of siRNA.

Furthermore, SNARE proteins can regulate ATP-sensitive potassium channels (K_{ATP}) which may play a key role in protecting against severe cardiac stress (e.g. myocardial ischemia and hypoxia; Chao et al. 2011). An example of this is when creatine kinase (enzyme involved in ATP regeneration) leads to an increased efflux of potassium ions leading to hyperpolarization of the cell membrane, in turn causing voltage-gated calcium (Ca_v) channel closure. This reduces Ca^{2+} influx (key factor in contraction) and consequently reduces contraction and energy consumption, resulting in 'protection' of the cardiac tissue (Chao et al., 2011). ANP has also

been shown to possess diuretic, natriuretic, and hypotensive attributes, as studied by their role to induce dilation in the heart, of arteries and veins (Saito 2010). With that said, there is yet scarce research mounted on SNARE proteins, the role they play in the mammalian heart, and more importantly, their expression and transcriptional regulation during development (Chao et al., 2011).

Without the seamless transport of proteins, lipids and other nutrients via vesicles from one cell to another (or more generally, an arbitrary donor and receiver of said nutrients), intracellular trafficking would not be possible. From within the cell, a given vesicle will be pulled, docked, and subsequently have its contents released for further cellular signaling (via fusion of various SNARE proteins; Sudhof & Rothman, 2009). Different SNARE proteins play different roles in the process of exocytosis, and their interaction is crucial to proper cellular functioning.

SNARE proteins can be broken down into two main categories: v-SNAREs (vesicle-bound) and t-SNAREs (target membrane bound) (Malsam & Söllner, 2011). Of importance to note is also a class of proteins called vesicle-associated membrane proteins (VAMP). Within a cell, v-SNAREs and t-SNAREs interact with one another at their SNARE motifs to form an alpha-helical complex (Duman & Forte, 2003). A heterotrimeric structure is formed between the VAMP (also referred to as synaptobrevin), syntaxin, and SNAP. In that configuration, the three-protein structure is in a *cis* conformation. Synaptotagmin (Ca^{2+} sensor) detects a localized increase of calcium ions, which in turn causes a conformational change from a *cis* configuration to a *trans* configuration in the aforementioned heterotrimeric structure (Maximov, Shin, Liu, & Südhof, 2007). This change causes the vesicle membrane to be pulled and fused to the cell membrane, and exocytose its contents (Hong, 2005). Throughout this process, another protein,

complexin, functions by mediating the fusion of the vesicle, and although it is not necessary, it increases neurotransmitter release by 60-70% as shown by mouse knockout (KO) of this protein (Hu, Carroll, Rickman, & Davletov, 2002; Jorquera, Huntwork-Rodriguez, Akbergenova, Cho, & Troy Littleton, 2012). Finally, NSFs and SNAPs function by undoing the alpha-helical complex, and 'recycling' the components for the next round of exocytotic release (Glick & Rothman, 1987).

A more recent classification of v-SNAREs and t-SNARES is that of R-SNAREs and Q-SNAREs, respectively. This classification system comes in part due to some SNARE proteins being localized on both vesicles and target membranes, as well as their structural differences (Burri & Lithgow, 2004; Malsam & Söllner, 2011). At the core SNARE complex, Q-SNAREs donate a glutamine residue whereas R-SNAREs donate an arginine residue. More specifically, at the main site of the SNARE complex, the zero ionic layer, R-SNAREs, like synaptobrevin, donate one arginine residue, while Q-SNAREs, like syntaxin and SNAP25, donate one glutamine residue (Fasshauer, Sutton, Brunger, & Jahn, 1998). These residues undergo dipole-dipole interactions around the zero ionic layer and form several other layers as the alpha-helical complex finalizes; since the zero ionic layer is at the center of this complex it is designated at layer 'zero' (Burri & Lithgow, 2004; Fasshauer et al., 1998; Malsam & Söllner, 2011).

The key SNARE proteins of this project are syntaxin 1A (STX1A) and SNAP25. The reason for that being is that often, they are expressed together to form a heterodimer (Dun, Rickman, & Duncan, 2010). These two proteins are at the core of all exocytotic releases, and although their role is crucial for proper intracellular trafficking, they must first be expressed in an organism, to help initiate exocytosis. In addition to interacting with one another, it has also been shown that their expression in the heart appears shortly after birth in mouse hearts (i.e. their

temporal expression mirrors one another). Thus, the transcriptional regulation on one might also be similar to the other (Peters et al., 2006).

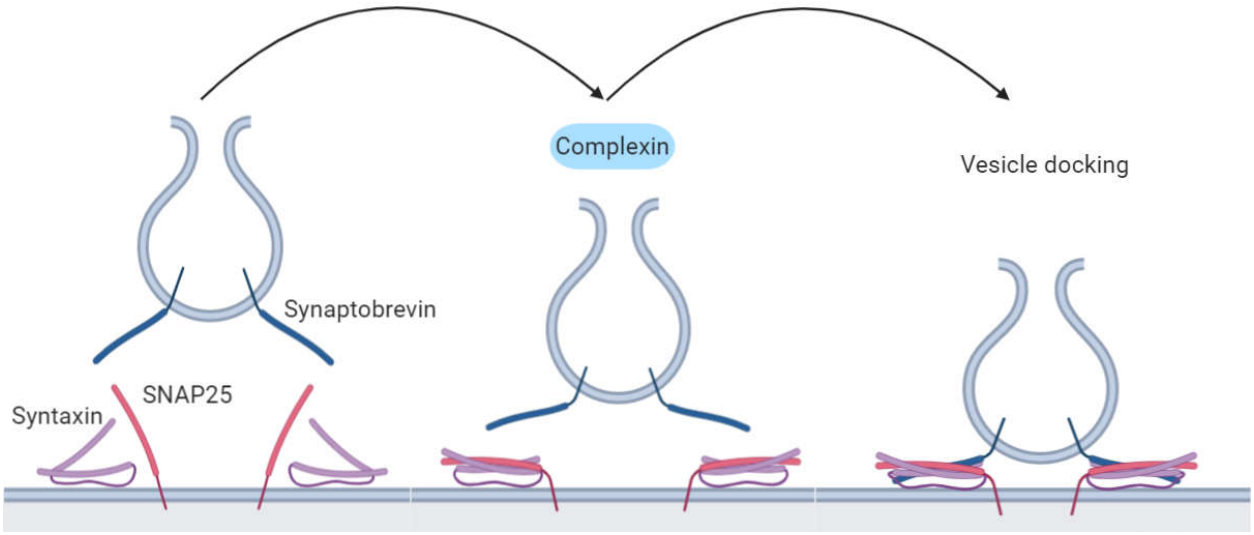

Figure 1: SNARE mediated exocytosis. Heterotrimeric structure forms between synaptobrevin, syntaxin, and SNAP25 to dock the vesicle to the cell membrane. Complexin acts as a mediator of the vesicle to help the vesicle dock faster (created with biorender.com).

Syntaxin 1A

Syntaxins, as part of the syntaxin protein superfamily (Rizo & Rosenmund, 2008), are encoded by respective STX genes (Thomas et al., 1988). Of note is the isoform STX1A; it has been studied more deeply in the brain as it is found in axon terminals for the regulated release of neurotransmitters. During calcium-regulated exocytosis, STX1A is responsible for the docking of vesicles to the presynaptic membrane. Syntaxins will bind with synaptotagmin and interact with voltage-gated Ca^{2+} and K^{+} channels (VGCCs and VGKCs, respectively) to help facilitate synaptic exocytosis. While synaptotagmin is responsible for the detection of Ca^{2+} via VGCCs, potassium channels (K_v) will ensure the repolarization of the membrane potential in facilitation of exocytosis (Feinshreiber, Singer-Lahat, Ashery, & Lotan, 2009). K_v channels will induce exocytotic release via depolarization of the membrane in direct interaction with syntaxin. These steps lead to vesicle fusion with the plasma membrane, and the vesicle will then be able to release its contents out of the cell for further cellular signaling. Recent studies, however, have shown that its expression is also found in cardiac myocytes and found to play a role in heart ion channel regulation as well (Ferlito et al., 2010; Peters et al., 2006). According to Peters and colleagues (2006), prior to their study, STX1A has mostly been observed in the brain, however, its more recent discovery of expression in cardiac myocytes has been shown to play a key role in exocytotic processes of the heart. Their study shows that STX1A is in fact expressed in adult cardiac myocytes, but not neonatal myocytes. The same study also showed that STX4 is involved in the exocytotic release of ANP granules in the heart of neonatal and adult mice, as well as STX4 being expressed in both neonatal and adult hearts (Peters et al., 2006). STX1A is hardly expressed in neonatal heart, but it has been found to be abundant in adult cardiac tissues, and SNAP25 and STX1A have both been found to be expressed in adult rat ventricular myocytes

(Chao et al., 2011). This discovery of SNAP25 and STX1A in these cardiac cells, proves that there is enough mounting evidence of SNARE expression in the heart; yet their exact mechanisms are yet unknown.

The importance of STX1A has been studied to have a direct expressional correlation to intelligence in Williams syndrome (Gao et al., 2010). This genetic disorder occurs when there is a spontaneous deletion of genetic material on chromosome seven, where the syntaxin gene is also located, such that the person is hemizygous for that gene. Some of the more serious complications of this disorder include heart problems and a time period of high blood calcium (Galaburda, Holinger, Bellugi, & Sherman, 2002). The Q-SNARE, STX1A, has been linked to learning and memory deficits in those with Williams Syndrome, solidifying its stature as a crucial protein and constituent in the formation of the SNARE protein complex (Gao et al., 2010).

SNAP25

Another Q-SNARE, SNAP25 interacts with synaptobrevin and STX1A to help form the SNARE complex, by each contributing an α-helix (Hong, 2005). SNAP25 will inhibit L- (skeletal and cardiac myocytes), Q- (cerebellar cells), and P-type (GABAergic Purkinje cells) VGCCs, and interact with synaptotagmin's domain without the help of Ca^{2+} (Chapman, 2002; Verderio et al., 2004). When it is expressed, SNAP25 can appear in two different isoforms, SNAP25A and SNAP25B (Nagy et al., 2005; Shimada et al., 2007). These isoforms differ in both expression as well as functional activities. Whereas SNAP25A is abundant in embryonic mouse brain and adult neurosecretory cells, SNAP25B is more predominant in adult neural tissue and during the major period of synaptogenesis, with minimal expression during development

(Shimada et al., 2007). Both SNAP25 isoforms are expressed from a single gene by alternative splicing of exon 5 (Ryabinin, Sato, Morris, Latchman, & Wilson, 1995). SNAP25 is crucial and vital for mammalian development, as studies have shown SNAP25 KO results in murine neonatal lethality (Jeans et al., 2007; Shimada et al., 2007). Like STX1A, SNAP25's expression has also been found in adult cardiac myocytes (Peters et al., 2006).

Heterozygous deletion of SNAP25 leads to the inconsistent regulation of synaptic Ca^{2+} levels and has therefore been linked to attention deficit hyperactivity disorder (ADHD; Brophy, Hawi, Kirley, Fitzgerald, & Gill, 2002; Mill et al., 2002). SNAP25 heterozygous mice treated with Dexedrine (active ingredient in Adderall - ADHD medication) showed a reduction in hyperactivity. STX1A and SNAP25 are crucial in both the development and functioning of a living organism. Understanding the underlying transcriptional machinery of these proteins will help shed light on to their expression and role in the developing heart.

Transcriptional Mechanisms

For gene expression to occur, DNA must first be copied into messenger RNA (mRNA) by RNA polymerase (Figure 1) during a process termed transcription. The newly formed mRNA sequence will leave the cell nucleus into the cytoplasm and serve as a template for protein synthesis, also known as translation. Gene expression is governed by its own set of regulatory elements that will increase or decrease the production of gene constituents. These regulatory elements are called transcription factors (TFs); they can act as either repressors or enhancers, in essence increasing or decreasing the expression of one or more genes (Frietze & Farnham, 2011; Waby, Bingle, & Corfe, 2008). There, TFs carry out their regulatory function through binding of respective sites located in the promoter region. The promoter region is located near the

transcription start sites of genes, on the same strand, and upstream of the gene (Shimada et al., 2007).

Transcription is initiated at the TATA box, a repeating thymine and adenine sequence located in the promoter region of a gene. To begin, a subunit of transcription factor II D (TFIID), called TATA-binding protein (TBP) binds to the TATA box causing a bend in the promoter sequence. From there, TBPs of other general TFs (e.g. TFIIA, TFIIB, etc.) will be recruited along with their respective general TFs to form the transcription pre-initiation complex (Dynlacht, Hoey, & Tjian, 1991; Louder et al., 2016). This newly formed complex, in combination with RNA polymerase II will begin RNA synthesis. Distal control elements found further upstream will interact with sequences of the promoter to induce expression of a gene. This is of note, as two genes can have the same promoter, but different distal control elements will yield different gene expression, depending on which part of the promoter TFs bind to, and therefore enhance or repress gene expression (Frietze & Farnham, 2011; Mandon, Nielsen, Kishore, & Knepper, 1997; Ryabinin et al., 1995)**.** While the TATA box is the transcription initiation site of most DNA sequences, some proteins do not have a TATA box, as is the case for STX1A, making it a TATA-less promoter. When a DNA sequence lacks a functional TATA box, the downstream promoter element (DPE) and initiator element (Inr) instead bind to TFIID, followed by recruitment of other general TFs and RNA polymerase II, in order to initiate transcription in a TATA-less promoter (Louder et al., 2016; Nakayama, Mikoshiba, & Akagawa, 2016).

Although all TFs play their own role, specificity protein (Sp1) deserves special mention, among other TFs (e.g. CREB, HIF, etc.), especially in the case of epigenetic regulation. Cai and colleagues (2008) were able to show that over-expression of Sp1, increases SNAP25 gene

expression, while conversely, inhibition of Sp1 transcriptional activation reduced SNAP25 gene expression, showing that it acts as a positive regulator. In a paper by Nakayama and colleagues (2016), it was shown that Sp1 is also a positive regulator of STX1A. Being a TATA-less gene, STX1A relies on the presence of Sp1 sites (as well as GC sites) in the promoter region for functional epigenetic changes. They have shown this by mutating one or both Sp1 binding sites, resulting in diminished STX1A promoter activity in PC12 cells (pheochromocytoma cells – an adrenal gland tumor cell line). They further confirmed the importance of Sp1 by transfecting SL2 cells (*Drosophila* cells deficient in Sp family of TFs); this resulted in a 2-fold increase in the STX1A core promoter region. Likewise, inhibition of endogenous Sp1 expression in the PC12 cell line resulted in about a 50% decrease in STX1A promoter activity compared to the control (Nakayama et al., 2016). Sp1 is but one of many TFs, but it nonetheless serves a crucial role in the expression of SNAP25 and STX1A, thus it deserves sole mention.

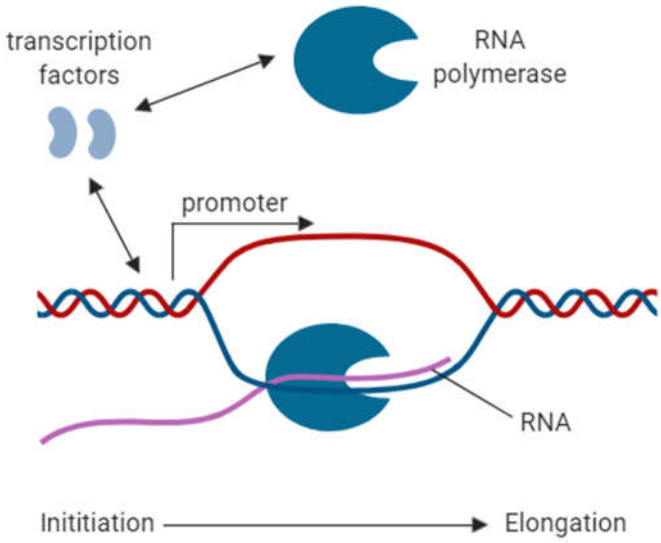

Figure 2: Simplified diagram showcasing TFs at work. Visible is the promoter region which is responsible for initiating gene transcription, and the various TFs at play in aiding this process (created with biorender.com).

Epigenetic Regulation of Cells

While a large portion of trait expression is due to heritable genetics, there are also epigenetic factors which can alter the phenotype without alteration in the DNA sequence; that is, they will be heritable in the short term, without causing genetic mutations. More generally, epigenetics are changes in organisms due to modifications in gene expression, as opposed to the alteration of the genetic code itself. Other times, there are also heritable epigenetic changes via DNA methylation, as methylation can change the activity of a DNA segment without causing any change in the sequence itself. This is done by the addition of a methyl group to a DNA molecule, on the two of the four DNA bases, cytosine and guanine. This process of DNA methylation largely functions to repress a gene, and for the most part, this methylation process is silenced when following its trajectory from parents to offspring, but that is not always the case (e.g. carcinogenesis, genomic imprinting). Various studies have also looked at the effects of transgenerational epigenetic inheritance of genes in humans, as was the case of the Dutch Famine of 1944, where offspring born during the famine were sizably smaller than the offspring before the famine. Overall, epigenetic changes refer to short-term changes in a cell or organism to alter gene expression.

The way this is done is through the remodeling of chromatin (Kaneda et al., 2005; Kubicek, Gilbert, Fomina-yadlin, Gitlin, & Yuan, 2012; Yoshida & Horinouchi, 1999). This dynamic modification of chromatin exposes highly condensed DNA to the regulatory transcription machinery of the cell (i.e. TFs). With the help of enzymes, chromatin can be altered to be more densely packed (heterochromatin), or to have a looser conformation (euchromatin); this is achieved via histone acetyltransferases (HATs) or histone deacetylases (HDACs), respectively. The presence of HATs, involves the addition of an acetyl group, increasing DNA

accessibility via a relaxed chromatin. On the other hand, HDACs remove acetyl groups from a histone, causing the DNA to tightly coil around the histone (Figure 2). As euchromatin, TFs are more readily able to access immediate early genes, since more of the DNA is exposed, thereby, increasing expression of a gene (Whittle & Singewald, 2014).

Trichostatin A

Among the many means of epigenetic regulation, one of the most used methods is via HDAC inhibition (Hakami, Dusting, & Peshavariya, 2016; Song, Liu, Li, An, & Tian, 2017; Wood, Rymarchyk, Zheng, & Cen, 2018; Yoshida & Horinouchi, 1999). A condensed chromatin yields transcriptional repression and such a structure is regulated by HATs. When an HDAC inhibitor is present, it functions by relaxing the chromatin structure, thereby giving access to immediate early genes for TFs to help drive expression. There are HDACs which function solely on specific histones (e.g. H2A or H2B), but in some cases, HDACs can function on a more global scale and inhibit all HDACs present, as is the case with trichostatin A (TSA).

Widely and consistently used for its ability to inhibit class I and II HDACs (Kubicek et al., 2012; Nakayama et al., 2016; Whittle & Singewald, 2014; Yoshida & Horinouchi, 1999), the inhibition of HDACs by TSA results in some major epigenetic changes within a cell. It has been observed that inhibition of HDACs results in muscle cell size increase (Iezzi et al., 2004; Kaneda et al., 2005). This change is of note with multipotent cell lines (i.e. H9c2) as for them to differentiate into muscle cells, some of the earliest signs fall on the presence of multi-nucleated cells, followed by the formation of myotubes, a crucial step in skeletal myogenesis. An equally important observation is in fact that the HAT induced activation of the CREB-binding protein (CBP) was found to play an important role in the hypertrophy of cardiac cells (Kaneda et al., 2005; Zhang et al., 2002). Zhang and colleagues found that while class II HDACs prevent

cardiac hypertrophy, the administration of HDAC inhibitors such as staurosporine, among others, caused rat hearts to show an increased cardiac mass. This is of note, as the present study aims to tap into the cardiac-like properties of H9c2 cells in order to get them to express cardiac markers.

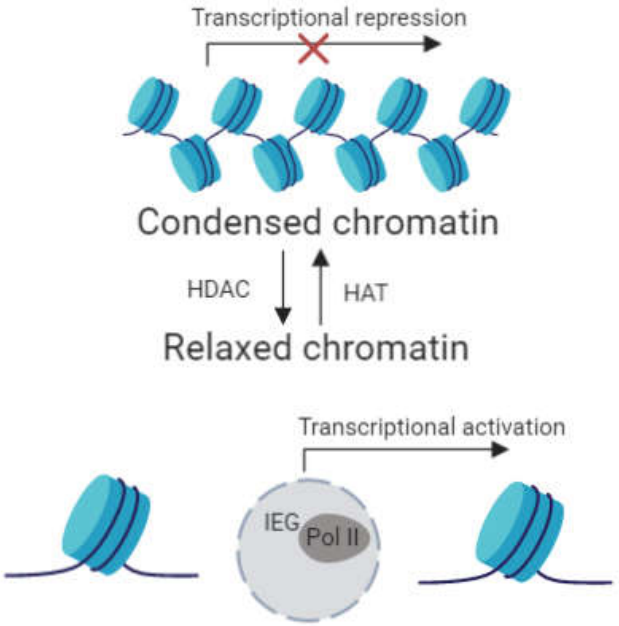

Figure 3: Histone acetylation and deacetylation under the effects of HAT and HDAC, respectively. Under HAT, immediate early genes (IEG) can be accessed by TFs to help drive expression of a gene (created with biorender.com)

Forskolin

Another method for altering gene expression is via the adenylyl cyclase pathway (Branco et al., 2015; Maximov et al., 2007). When intracellular levels of cyclic adenosine monophosphate (cAMP) rise, it acts as a secondary messenger to signal protein kinase A (PKA) via cAMP-sensitive pathways. This increase in PKA directly activates cAMP response element-binding protein (CREB) which in turn binds to cAMP response element (CRE) located upstream within the promoter. This binding along with the conversion of ATP to ADP causes transcriptional activation, thereby altering gene expression. The drug forskolin (FOR) functions by activating the enzyme adenylyl cyclase which directly increases intracellular cAMP, causing the above-mentioned cascade of events.

The ability to epigenetically regulate cAMP levels is a key feature of FOR as its application in vitro has been shown to have not only similar effects to isoproterenol (a drug used to treat bradycardia) but almost to the same extent, in the cardiac-like cell line, H9c2 (Hescheler et al., 1991). This was done in order to stimulate the ß-adrenergic pathway of H9c2 cells using either FOR, or intracellular addition of cAMP (Hescheler et al., 1991; Yoo et al., 2009). It has been previously shown that PKA-mediated phosphorylation of the cardiac proteins (e.g. L-type VGCC, ryanodine receptor, phospholamban, cardiac myosin binding protein-C (cMyBP-C) and cardiac troponin I (cTnI)) was correlated with ventricular contractility, in both primary ventricular tissue, as well as ventricular tissue-derived cardiac cells (Hanft et al., 2016; Hescheler et al., 1991). For the present study, FOR will also be applied to H9c2 cells in order to stimulate intracellular cAMP via adenylyl cyclase, in the hopes of inducing expression of SNARE proteins, and due to the multipotent nature of these cells, any other skeletal or cardiac biomarkers.

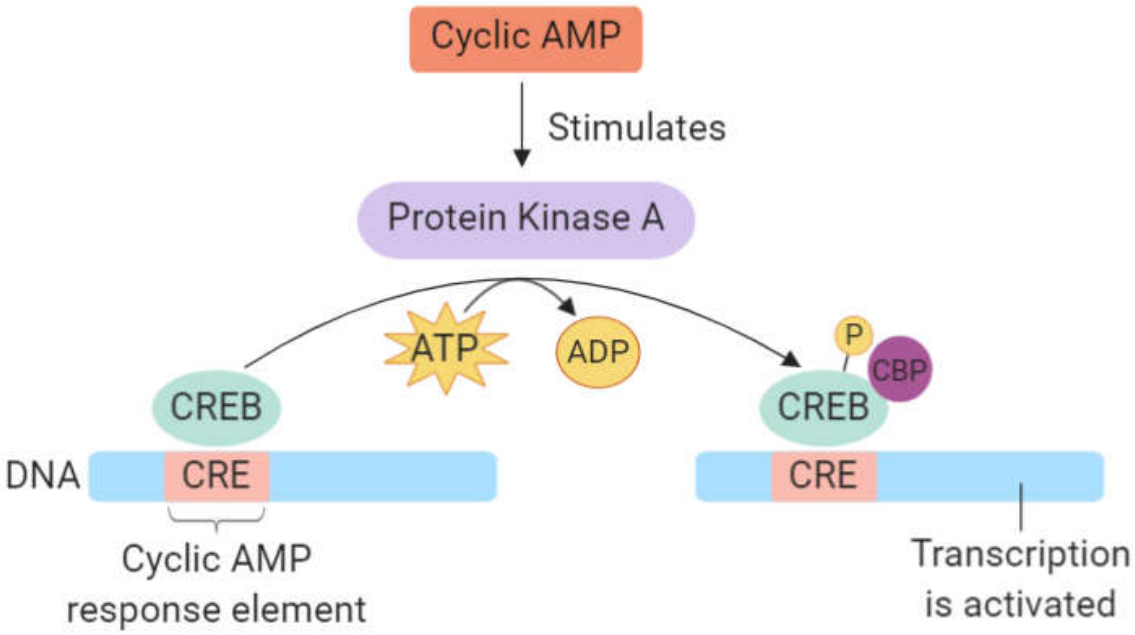

Figure 4: Diagram showcasing cyclic AMP activation. FOR activates the enzyme adenylyl cyclase and increases intracellular levels of cyclic AMP, which in turn stimulates PKA. This PKA stimulation causes CREB to bind to the cyclic AMP response element with the aid of ATP and allow for downstream signaling (created with biorender.com).

Retinoic Acid

One benefit of working with multipotent cells is the ability to not only observe their phenotypic changes, but also observe intracellular changes, mRNA and protein expression, as they undergo differentiation. Although there are many routes of achieving differentiation, a potent differentiating drug, and one used often throughout literature is retinoic acid (RA) (Branco et al., 2015; Menard et al., 1999; Parameswaran, Kumar, Verma, & Sharma, 2013; Pereira et al., 2011; Sucharov, Langer, Bristow, & Leinwand, 2006; J. Zhang et al., 2015). A fat-soluble and vitamin A metabolite, RA functions by entering the nucleus of a cell, binding to the already present retinoic acid receptors (RAR) which are nuclear receptors, where transcription takes place (Zhang et al., 2015). Briefly, RA functions by repressing pluripotency-associated genes, in essence 'forcing' the cell to differentiate into one type or another (Zhang et al., 2015). It also functions by altering RNA sequences, and other epigenetic modifications such as DNA and histone methylation, and histone acetylation.

As a type II nuclear receptor, RAR heterodimerizes (formed by two different proteins) with another nuclear receptor, retinoic X receptors (RXR) via non-covalent bonding. In the absence of a molecular ligand, the newly formed RAR-RXR heterodimer will bind to already present hormone response elements on a DNA strand, known as retinoic acid response elements. When a ligand agonistically binds to RAR, the present corepressor protein found on RAR dissociates, and cause the recruitment of a coactivator protein instead. This newly present coactivator will drive transcription of the respective downstream target gene. Finally, as mentioned above, RAR gene expression is under regulation by gene promoter methylation and acetylation.

With the cell line used for this study being known to exhibit multipotent characteristics, previous research has set out to differentiate H9c2 cells due to their ability to become either cardiac or skeletal muscle cells (Branco et al., 2015; Menard et al., 1999; Watkins, Borthwick, & Arthur, 2011). Successful differentiation using 10 nM of RA had resulted in an enhanced expression of cardiac L-type VDCCs, while at the same time, a reduced expression of skeletal VDCCs and myogenin, a skeletal muscle differentiation marker (Menard et al., 1999), going to show that H9c2 cells tended towards a more cardiac than a skeletal phenotype. RA will be used in vitro, in order to induce differentiation of H9c2 cells towards a cardiac phenotype, and measure SNARE protein expression, alongside cardiac biomarkers like cardiac troponin T (cTnT).

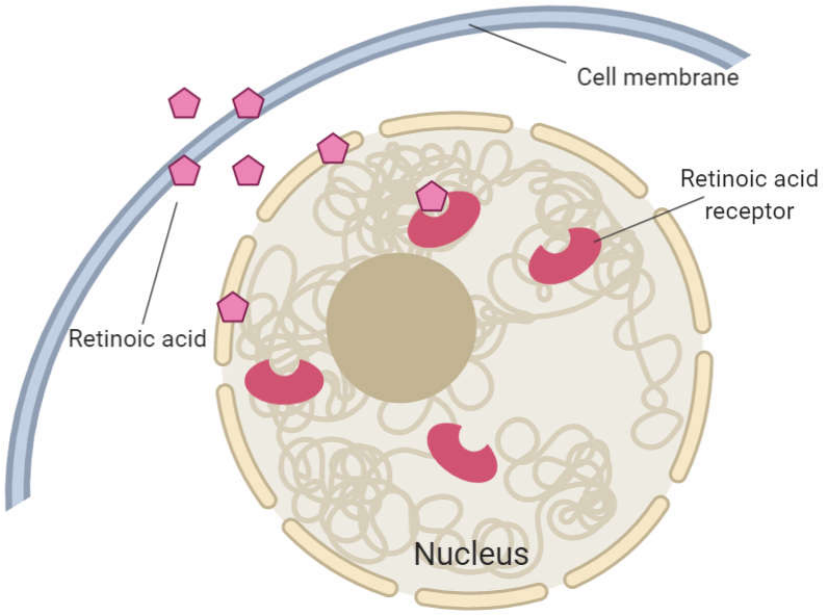

Figure 5: Retinoic acid binds to retinoic acid receptors in the nucleus in order to promote transcription, and force multipotent cells down a specific pathway (created with biorender.com)

INS-1 832/13 Cell Line

The present study set out to determine SNARE protein expression in a H9c2 cells, but it should be noted these cells are not true cardiac cells compared to primary neonatal or adult cardiomyocytes. Not only that, but H9c2 cells do not endogenously express SNAP25 nor STX1A. A second cell line was selected for this study called INS-1 832/13, for a couple of reasons; first, the INS-1 cell line endogenously expresses SNAP25 and STX1A, and secondly, they were selected to assess baseline expression of the two SNARE proteins against H9c2 cells. INS-1 is a rat insulinoma cell line, derived from specialized beta islet cells that continuously secrete insulin, resulting in hypoglycemia (Burns & Edil, 2012). This characteristic has made them an attractive choice for studies wanting to look at the effectiveness and screening of diabetes drugs, as well as a model for insulin secretion regulation, and pancreatic islet ß-cell function (Hectors, Vanparys, Pereira-Fernandes, Martens, & Blust, 2013; Hohmeier et al., 2000; Lorenz, El Azzouny, Kennedy, & Burant, 2013; Salunkhe et al., 2017).

INS-1 cells, however, have a glucose-stimulated insulin secretion (GSIS), that may decrease over time, as such, the INS-1 832/13 cell line was derived from the original INS-1 cell line. This new cell line has been selected for its more robust GSIS, but also because it secretes both rat and human insulin (Hectors et al., 2013). Due to the insulin secreting nature of INS-1 cells, they endogenously express SNAP25 and STX1A; two necessary proteins for the exocytotic release of insulin from vesicles. (Burns & Edil, 2012; Hectors et al., 2013; Jeans et al., 2007; Kubicek et al., 2012; Lorenz et al., 2013; Salunkhe et al., 2017). They also exhibit a robust sensitivity to potassium as they contain an abundance of ATP-sensitive K^+ channels. Since potassium is highly critical to the permeability of ß cells, this could be another reason why this cell line is selected for studies wanting to look at the secretion of insulin and the effectiveness of

drugs on reducing hypoglycemia. In this study, INS-1 832/12 cells were used in order to assess baseline promoter activity with relation to H9c2 cells, as well as for positive controls in western blotting due to their expressing of SNAP25 and STX1A. It was also prudent to observe how H9c2 cells' gene promoter regulation of SNAP25 and STX1A compares to the gene promoter regulation of a cell line that already has the transcriptional machinery to express these two SNARE proteins.

H9c2 Cell Line

The main goal of this study was to examine the regulatory mechanisms of SNAP25 and STX1A expression in the heart. For this reason, it was important to select a cardiac model that would be relatively easy to culture and work with in vitro. True cardiac myocytes do not proliferate in vitro and are very difficult to maintain. Thus, the choice for this study shifted towards a cardiac-like cell line called H9c2 (Figure 5). This cell line is derived from the lower half of 13-day old embryonic rat heart, consisting mostly of ventricular tissue and it is known to replicate, but will not contract in vitro (Parameswaran et al., 2013). Their phenotype resembles that of skeletal muscle cells, as well as ventricular primary myocytes, but tend to have a more skeletal muscle cell affinity. H9c2 cells have also been shown to share electrophysiological characteristics and respond to G-protein signaling like adult cardiac myocytes (Hescheler et al., 1991). Hescheler and colleagues built their experiment upon a different study (Kimes & Brandt, 1976) that was able to show H9c2 cells adopted features of skeletal muscle because the cells expressed nicotinic receptors (role in baroreflex) and synthesized a muscle-specific creatine phosphokinase (ATP regeneration).

H9c2 cells have also been shows to respond to drug treatments on the ß adrenergic pathway similarly to cardiac cells. When FOR was added in vitro, and more specifically, when cAMP was increased intracellularly (with or without FOR), researchers found an increase in the expression of cardiac VDCCs (Florea & Cohn, 2014; Menard et al., 1999). Along the same research, they have been found to show similar cardiac hypertrophic responses to primary neonatal cardiac myocytes. A study by Branco and colleagues found that when H9c2 cells were treated with angiotensin, they exhibited a rearrangement of contractile proteins and an upregulation of hypertrophic genes similar to primary neonatal cardiac myocytes (Branco et al., 2015; Watkins et al., 2011).

Being derived from fetal ventricular tissue, H9c2 cells are multipotent. They can take on either a cardiac or a skeletal muscle phenotype (Figure 7), as previous research has shown (Branco et al., 2015; Hernandez-Gonzalez et al., 2006; Parameswaran et al., 2013; Pereira et al., 2011; J. Zhang et al., 2015). When exposed to certain drug treatments, such as RA, H9c2 cells' multipotency genes get silenced, and they are forced towards a specific phenotype. Coupled with the drug treatment, a reduction in the concentration of fetal bovine serum (from 10% to 1%), takes them from a proliferative state to a differentiated state. Other research has shown that replacing fetal bovine serum with fetal horse serum can have a similar effect on the transition from proliferative to differentiated state, however, a reduced bovine serum concentration seems to be enough to yield the same results (Branco et al., 2015; Pereira et al., 2011; Ruiz et al., 2012).

Since primary cardiac cells are difficult to maintain in vitro (i.e. they do not proliferate and cannot be passaged), H9c2 cells can be a suitable alternative as ultimately, they are derived from embryonic ventricular tissue and, given the right circumstances, have the capability to develop into cardiac cells (or skeletal muscle cells). Differentiation of these cells via various

means (i.e. reduced FBS serum, retinoic acid treatment) takes them to a state akin to neonatal cardiac cells. From this state, one could observe how they could mimic the maturation of neonatal cardiac cells to adult cardiac cells. These findings lend heavy support to the versatility H9c2 cells pose as a cardiac alternative to primary cardiac cells, which is what led to them being the top choice for this study.

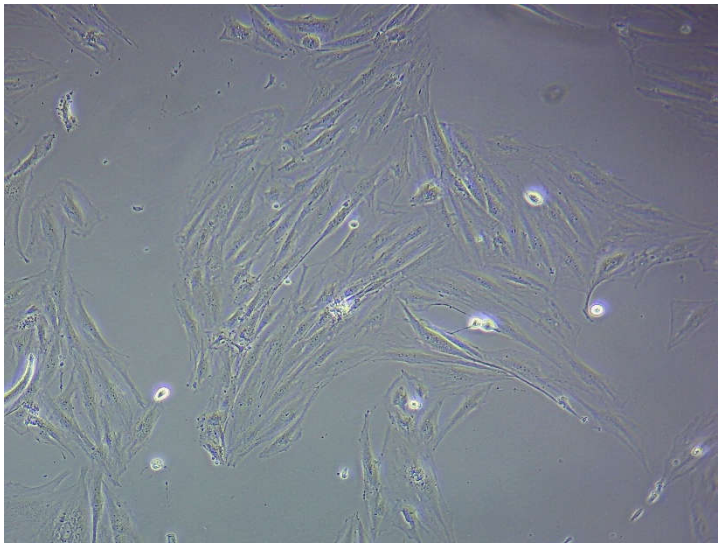

Figure 6: H9c2 cells in their undifferentiated state. The cells are present as single-nucleated cells, and are multipotent in this state, capable of taking on a more cardiac or skeletal muscle phenotype.

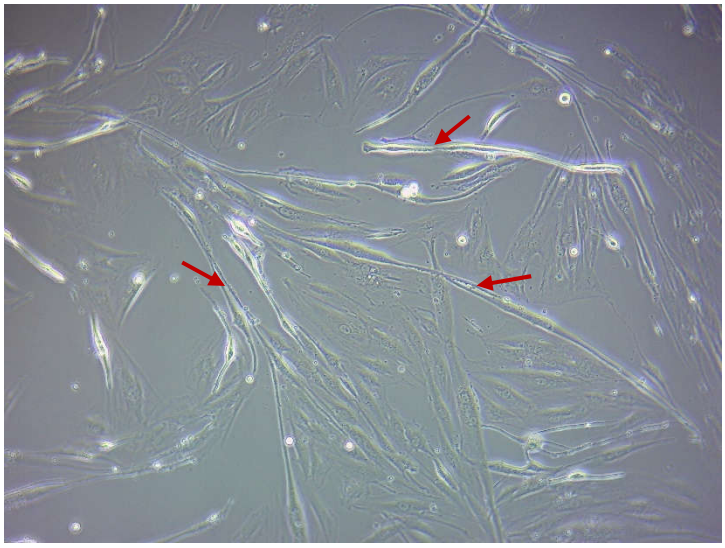

Figure 7: H9c2 cells that have been differentiated by RA and reduced serum media. Present are multi-nucleated cells in the form of myotubes (highlighted by the red arrows), an early precursor of myogenesis which will lead to the formation of skeletal muscle fibers.

Purpose and Hypotheses

There has been mounting evidence to suggest that the heart does not solely function as a pump for blood, but rather, also as an endocrine organ, with the likes of ANP and BNP secretion acting to maintain extracellular fluid volume and blood pressure. For these to occur, STX1A and SNAP25 may be necessary for the exocytotic release of these hormones, among other vesicular contents. As mentioned previously, Peters and Ferlito (Ferlito et al., 2010; Peters et al., 2006), found SNARE expression in adult rat hearts. In addition, unpublished results from the Tsushima lab also found adult rat SNARE expression, but neither Peters, Ferlito, nor the Tsushima lab were able to ascertain SNARE expression in a neonatal cardiac model. The underlying mechanisms for the differences between adult rat heart and neonatal rat heart have not been established.

For the purpose of this study, the cell line H9c2 were used as a cardiac model alternative. The choice of this cell line comes from their potential to model neonatal cardiac myocytes, as they were originally derived from embryonic ventricular rat tissue. Differentiation of these cells using retinoic acid and low FBS might mimic the maturation of heart cells going from neonatal to adulthood.

As such, the goal of this study was to examine the transcriptional machinery of SNARE protein expression in a cardiac model. In order to do this, the promoter activity and expression of SNAP25 and STX1A was tested in the H9c2 cell line. Promoter activity was assessed in both untreated H9c2 cells, as well as cell batches treated with TSA or FOR, or cells differentiated with RA. Since H9c2 cells do not endogenously express SNAP25 and STX1A, they were transfected with promoter constructs of those two SNARE proteins. The full-length and truncated promoter constructs could shed insight into whether the developmental changes in

STX1A and SNAP25 expression in the heart is at the transcriptional level or due to epigenetic regulation.

Luciferase reporter assays were used to assess promoter activity by transfecting pGL3 luciferase plasmids that contain full length and truncated regions upstream of STX1A and SNAP25 and a Renilla luciferase construct as an internal control. The choice for this plasmid vector comes from its lack of promoter/enhancer sequences. In other words, expression of the luciferase coding region it contains depends on a functional promoter being inserted upstream of the luciferase complementary DNA in the multiple cloning site. These full-length and truncated regions used for transfection in this study were obtained from two papers that have already established the CPR of STX1A and SNAP25. The STX1A gene promoter constructs were obtained from Nakayama and colleagues (2016), and the SNAP25 gene promoter constructs were obtained from Shimada and colleagues (2007).

With regards to H9c2 cell differentiation, the mechanisms underlying RA treatments are still being studied, however, it has been shown that RA treatment causes differentiation by altering encoding RNA sequences, thereby altering expression of the cell (Zhang et al., 2015). Transfection with the same promoter constructs was also performed on INS-1 cells, along with a luciferase reporter assay in order to assess and establish a baseline promoter activity, determine the potential maximal gene reporter activity for SNAP25 and STX1A, and compare that to the promoter activity of H9c2 cells.

The hypothesis is that treatment via TSA and FOR will yield higher SNAP25 and STX1A promoter activity and induce the expression of SNAP25 and STX1A in H9c2 cells. It is also hypothesized that differentiation of H9c2 cells via RA will induce expression of SNAP25 and STX1A proteins, and that they will differentiate towards a cardiac phenotype. These experiments

should help lend validity and illuminate the underlying mechanisms of SNARE proteins in the mammalian heart.

Materials and Methods

Cell Culturing

H9c2 cells were obtained from Sigma-Aldrich (Oakville, ON) and were cultured in either 100 mm single dishes, 6-well 9.6 cm^2, or 12-well 3.5 cm^2 plates, depending on whether they were drug treated or transfected. INS-1 832/13 cells were obtained from Dr. Christopher Newgard (Duke University, Duke Molecular Physiology Institute) and were cultured in 100 mm single dishes, 6-well 9.6 cm^2, or 12-well 3.5 cm^2 plates. Both cells lines were incubated at 37°C and 5% CO_2. H9c2 cells were grown and cultured in Dulbecco's Modified Eagle's medium (DMEM; MilliporeSigma), supplemented with 10% fetal bovine serum (FBS; ThermoFisher) and 1% penicillin-streptomycin (PS) (to 500 mL DMEM). INS-1 832/13 cells were grown and cultured in Roswell Park Memorial Institute (RPMI; MilliporeSigma) 1640 medium, supplemented with 10% FBS, 1% PS, 50 µM sodium pyruvate, and 2.17 µL ß-Mercaptoethanol (to 500mL RPMI).

Cell Passaging

H9c2 and INS-1 832/13 cells were passaged when they reached approximately 80% confluency. All passaging steps were performed in a tissue culture hood under sterile conditions. Prior to passaging, the hood was sprayed with 70% ethanol, and a UV light was used to sterilize the environment for 15 min. Once the hood was sterilized, the culture dishes were placed in the hood for passaging. The cell media was removed and discarded, and cells were washed with 1x Phosphate Buffered Saline (ThermoFisher; PBS) solution to remove any remaining media. Since the cells were grown in a monolayer, the PBS solution was placed around the edge of the culture dish(es) to not disturb the adhered cells. The dish was then manually rocked back and forth to

allow the PBS solution to wash over the cell monolayer and to rinse any leftover media, before being removed and discarded. A 0.25% trypsin solution (diluted from 2.5%; ThermoFisher) was added to the culture dish to cleave the proteins causing the cells to adhere to the dish, therefore causing the cells to detach from the plate. Enough trypsin solution was added to cover the bottom of the bottom of the culture dish (~3 mL for a 100 mm dish). The dish was incubated at room temperature for 2-3 min., and their detachment was confirmed by viewing the dish under a light microscope. The cells/trypsin solution was then placed in a 15 mL conical centrifuge tube, with an added 1:1 volume of fresh media (for each respective cell line) to help stop the effects of the trypsin solution from cleaving the cells themselves. The cells were centrifuged at 2000 rpm for 2 min. at room temperature to pellet the cells. The trypsin/media supernatant was discarded, and the pellet was resuspended with fresh pre-warmed media. The cells were passaged between 1:2-1:4 depending on required growth rate and seeded in new 100mm dishes, 6-well, or 12-well plates, depending on their intended use (i.e. drug treatment, maintain cell line, or transfection).

HDAC Inhibitor Treatment

At 70% confluency, H9c2 cells were treated with trichostatin A (TSA) (MilliporeSigma), a potent HDAC inhibitor. Cells were passaged in 100 mm dishes for drug treatment and labeled according to the length and concentration of the drug treatment. Cells were treated for 24 hrs. with a TSA concentration of 10 μM. As per the manufacturer's instructions, the salt form of the drug was suspended in dimethyl sulfoxide (DMSO). The initial stock was 10 mM, and the prepared drug was suspended in fresh cell media. Since DMSO is quite viscous, the drug had to be vortexed in a tube of media before placing the mixture on the cell culture dish, to ensure even

coating of all cells in the TSA drug. The cells were incubated for 24hrs at 37°C after which they were lysed (see "cell lysis and preparation" section).

PKA Activation Treatment

At 70% confluency, H9c2 cells were treated with forskolin (FOR) MilliporeSigma), a known phosphokinase A activator (PKA). Cells were passaged and plated similarly to the TSA treatment in a 100 mm dish. The drug was prepared using DMSO as per the manufacturer's instructions, for a final concentration of 24 mM stock. The drug was diluted in media and vortexed for a final concentration of 10 μM on the cells; this ensured that the drug was evenly dispersed in the media and the cells were all able to receive the drug when applied to the dish. Cells were incubated at 37°C for 4hrs after which they were lysed (see "cell lysis and preparation" section).

Cell Differentiation

At 70% confluency, H9c2 cells were treated with 100 nM of retinoic acid (RA) to induce differentiation of the cell line towards a more cardiac phenotype, and less skeletal muscle type. The media composition was kept the same, however FBS was reduced from 10% to 1%. The RA was added to a tube of media, vortexed and then added to the 100 mm culture dish, for a final concentration of 100 nM of RA. The cells were incubated at 37°C for 6 days, RA was added daily, and media was replenished every 2 days. All steps that involved the handling of RA were performed in the dark, since RA is light-sensitive. The cells were then lysed and prepared for analysis (see "cell lysis and preparation" section).

Cell Lysis and Preparation

Both INS-1 832/13 and H9c2 cells were lysed by placing the dishes on ice. Media was removed and discarded, the dishes were rinsed two times with 1x PBS, and finally 1 mL of 2x SDS was added to lyse the cells. Using the back of micropipette tip, the bottom of dish was scraped evenly and thoroughly to ensure all cells were lysed. The lysed contents were transferred to microcentrifuge tubes, boiled at 100°C for 10 min., centrifuged at 12,000 g for 30 min. at 4°C, and the supernatant was transferred to a microcentrifuge tube for a protein assay and western blotting (Bradford-Lowry assay).

Bradford Assay

A Bradford protein assay was performed on lysed cells to determine protein concentration in the sample, using the DC Protein Assay Kit (Bio-Rad). This was done by creating a protein standard curve of 1, 0.5, 0.25, 0.125, and 0.0625 µg/µl BSA. The BSA standards and cell lysates were added to cuvettes along with Reagent A, B and S, and was left to incubate for 20 min at room temperature. A spectrophotometer was then used to measure the absorbance of the protein standards and lysed samples. The values were plotted on a graph, and using the obtained function, the lysed samples' protein concentration could be calculated to determine how much protein to load for a Western Blot.

Western Blotting

Lysed samples were prepared for western blotting, by adding SDS dye, as well as Milli-Q filtered water, to create appropriate dilutions for blotting. 1.5 mm, 12% gels were prepared using Milli-Q water, 30% acrylamide-bis, 1.5 M Tris (pH 8.8; running gel) or 1.0 M Tris (pH 6.8;

stacking gel), 10% SDS, 10% ammonium persulfate (APS), and TEMED. Appropriate amounts of protein samples were loaded into the wells of the solidified gels, along with 5 µL BLUelf Prestained Protein Ladder (Genedirex), including positive control for the protein blotted, and a control of untreated cells. Gels were resolved in a bath containing running buffer (25 mM Tris base, 190 mM glycine, and 0.1% SDS) with the help of an electroporator (Bio-Rad) for 1 hr. at 150V. Once the proteins were resolved, and ladder separated, a transfer "sandwich" was prepared by placing the gel on a nitrocellulose membrane (presoaked in transfer buffer; 25 mM Tris base, 192 mM glycine, and 20% methanol), sandwiched between two filter papers and two sponges; the transfer was run for 1 hr. at 100 V. Once the transfer was complete, the nitrocellulose membrane was washed in TBST wash buffer (20 mM Tris base, 137 mM NaCl and 0.1% Tween 20) 3x5 min. The membrane was then placed in blocking solution (20 ml water and 1 g skim milk powder; Bioshop) and rocked at room temperature for 1 hr. The blocking solution was discarded, and the membrane was washed 3x5 min again with TBST to remove any excess blocking solution. The appropriate primary antibody (STX1A, SNAP25, cTnT from Abcam, and MyoG from the McDermott lab, York University; Table 1) was added (10 µL antibody and 10 mL 1% BSA) to the membrane overnight. The following day, the membrane was washed once again 3x5 min with TBST, before the secondary antibody (10 mL sterile PBS, 10mL 1% BSA, and 4 µL antibody; Table 1) was placed on and rocked for 1 hr. at room temperature covered with aluminum foil to help preserve the secondary antibody as it is light-sensitive. The secondary antibody was removed, and four more washes were done, 1 x 15 min and 3 x 5 min, before the membrane was visualized at 700 nm and 800 nm channels using the LI-COR Odyssey B446 Infrared Imaging System (LI-COR).

Table 1: Primary and secondary antibodies used for western blotting, for each respective protein being blotted, along with their host and dilution factors.

	Host/Class	Source, Cat#	Dilution
Primary Antibodies			
Anti-syntaxin 1A	Rabbit, polyclonal	Abcam, #ab70293	1:1000
Anti-SNAP25	Rabbit, monoclonal	Abcam, #ab109105	1:1000
Anti-myogenin	Mouse, monoclonal	McDermott Lab, York University	1:20
Anti-cardiac troponin T	Rabbit, polyclonal	Abcam, #8295	1:1000
Anti-GAPDH	Mouse, monoclonal	Abcam, #ab8245	1:1000
Secondary Antibodies			
Anti-Mouse	Goat, polyclonal	LI-COR, #926-32210	1:10,000
Anti-Rabbit	Goat, polyclonal	LI-COR, #926-68071	1:10,000

Bacterial Transformation of STX1A and SNAP25

Using the bacterial strain *Escherichia coli* (*E. coli*) DH5α (Invitrogen), transformation was performed by adding 1μL of the pGL3 luciferase plasmid DNA vector (Figure 5), containing truncated lengths of the STX1A and SNAP25 promoter regions. The truncated lengths were obtained via a restriction enzyme digest, using HindIII for SNAP25 (Ryabinin et al., 1995), and MluI for STX1A (Nakayama et al., 2016), although this was not performed by our lab. The SNAP25 full-length and truncated regions of the gene promoter were obtained from Dr. Michael Wilson (University of New Mexico, Albuquerque, NM, USA) and Dr. JoAnne Richards (Baylor College of Medicine, Houston, TX, USA, while the STX1A full-length and truncated regions were determined and obtained from Dr. Takahiro Nakayama (Kyorin University School of Medicine, Tokyo, Japan).

The pGL3 luciferase vector consists of an ampicillin resistance gene, a luciferase reporter gene, and a multiple cloning site where the truncated promoter regions of STX1A or SNSAP25 were inserted (one construct per vector for a total of 12 individual *E. coli* batches). These promoter regions are located upstream towards the 5' end of the sense strand. The STX1A promoter sequences of interest were -1931, -1239, -627, -204, -88 and the SNAP25 promoter sequences of interest were -1517, -292, -102, -41, +22, +114.

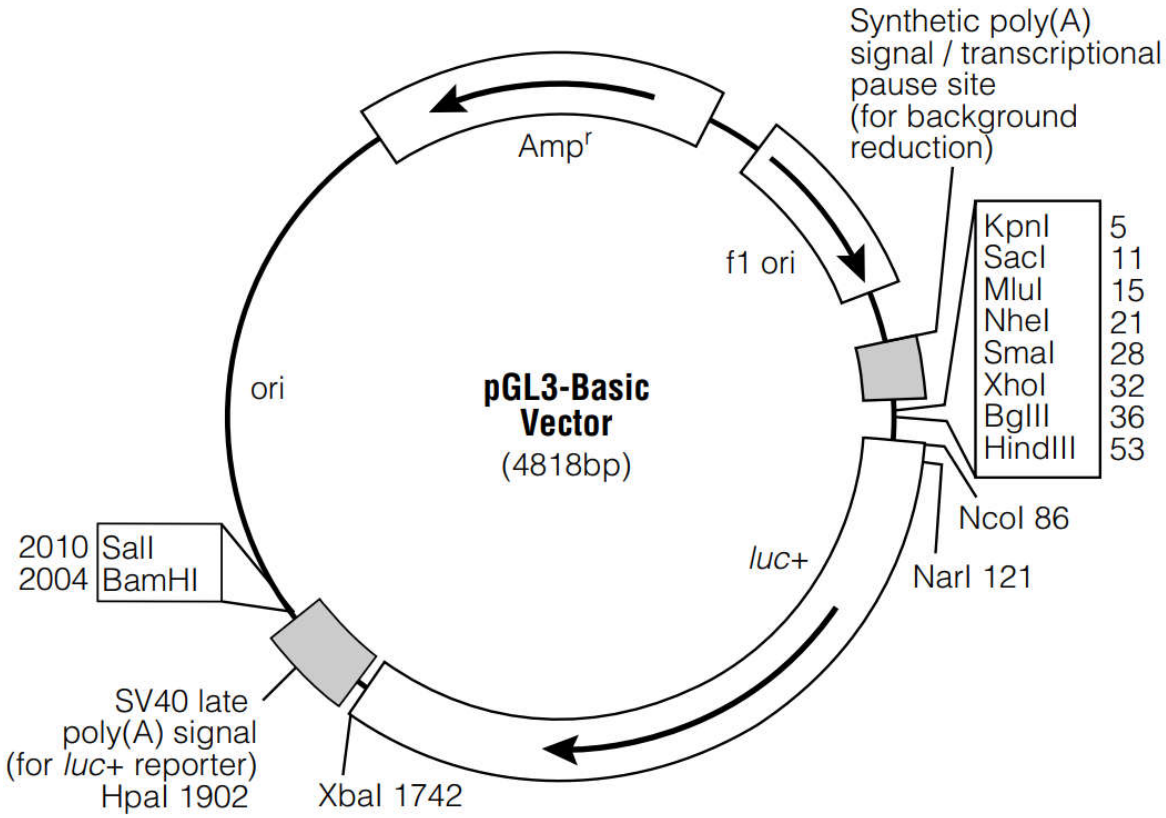

Figure 8: pGL3 Vector into which truncated regions were inserted. Upstream promoter regions were inserted in the multiple cloning site, immediately upstream of the luc+ gene, as the downstream luciferase reporter gene depends on this being present to create a signal (Promega).

Once the plasmid DNA was dispensed into the *E. coli*, the cells were incubated on ice for 30 min, heat-shocked for 30 secs in a 37°C water bath, and then back on ice for 2 min. The tubes were then placed in a 37°C orbital shaker for 1 hr. at 250 rpm. The now plasmid-containing *E. coli* were pipetted onto LB-agar petri dishes (LB broth, agar powder, and ampicillin; Invitrogen), and using a sterilized L-shaped cell spreader, the bacteria was uniformly spread on the petri dish, and were then incubated at 37°C overnight. The following day, bacterial growth was confirmed via colony growth after which enough LB media (LB broth base and water; Invitrogen) was aliquoted into a tube for colony isolation by plasmid construct; this step was performed near a flame (Bunsen burner) to create a vacuum effect and keep the contents of the LB media bottle sterile. 12 test tubes were labeled with one of the 12 constructs and 3 mL of LB media was added to each, along with 5% ampicillin. The petri dishes were removed from the incubator (plates that did not grow colonies signified plasmid take-up failure), and using a sterile inoculation loop, a single colony was swiped from the dish, and rinsed in the respective LB media tube. The tube tops were left semi-open (*E. coli* is aerobic) and were then placed overnight in a 37°C orbital shaker at 250 rpm. The next day, plasmid purification was performed.

Plasmid Purification, Isolation, and Quantitation

The 12 tubes (now cloudy from bacterial growth) were removed from the orbital shaker and prepared for plasmid purification. All steps were performed at room temperature using the PureLink HiPure Plasmid Miniprep Kit (ThermoFisher) and a centrifuge, and steps were performed as per the included instructions. Briefly, the *E. coli* were pelleted via centrifugation, LB media removed, and pellet resuspended in a resuspension buffer (50 mM Tris-HCl pH 8.0, 10 mM EDTA, RNase A). During this time HiPure Mini Columns were equilibrated with

equilibration buffer (10 mM Tris-Cl pH 8.5) and the buffer was left to dispense by gravity flow. Lysis buffer (200 mM NaOH, 1% SDS) was then added and tubes were incubated for 5min to lyse the bacteria, followed by precipitation buffer (3.1 M potassium acetate, pH 5.5). The tubes were centrifuged at 12,000 g for 10 min, and the supernatant was placed into the newly equilibrated columns and allowed to drain by gravity flow. Wash buffer (0.1 M sodium acetate, 825 mM NaCl) was added twice to the columns and allowed to drain by gravity flow. The filter of the columns allows the wash to pass through with proteins, RNA, and other impurities, while allowing the DNA to remain in the filter. After the washes, a sterile microcentrifuge tube was placed under the columns, and elution buffer (10 mM Tris-HCl pH 8.0, 0.1 mM EDTA) was added to the column and allowed to drain by gravity flow. Ice-cold isopropanol was added to the eluate and the new solution was centrifuged at 12,000 g for 30 min at 4°C. The supernatant was discarded and ice-cold 70% ethanol was added to the microcentrifuge tube and centrifuged once more at 12,000 g for 5 min at 4°C. The supernatant was removed once more, and the remaining pellet was left to air-dry for 10 min, before finally adding TE buffer (10 mM Tris pH 8.0, 1 mM EDTA). The remaining solution contained the purified plasmid DNA.

The isolated plasmids' DNA concentration was measured (in ng/µL) using a NanoDrop 2000 Spectrophotometer (ThermoFisher). Following blanking, a 2 µL sample of DNA from each isolated construct, was placed on the pedestal of the machine to measure absorbance at 260 nm and 280 nm. An absorbance ration A_{260}:A_{280} of ~1.8 meant that the sample was pure. Once all nucleic acid concentrations were obtained, the samples were used for cell transfection (see Cell Transfection).

RNA Isolation and Quantitation

In order to isolate RNA, H9c2 and INS-1 832/13 cells were passaged and plated on 100 mm dishes and allowed to adhere overnight before proceeding with the respective treatments. H9c2 cells were treated with either TSA, FOR (see HDAC Inhibitor and PKA Activation treatment sections in Methods) or transfected with Sp1 plasmid DNA (see Cell Transfection). For the RNA isolation, the PureLink RNA Mini Kit (ThermoFisher) was used. Growth medium was removed, and trypsin was added to the cells in order to remove them from the plate. The cells were placed in an RNase free tube and centrifuged at 2,000 g for 5 min. The growth medium and trypsin were discarded, appropriate volume of lysis buffer (10 mM Tris pH 7.4, 0.25% Igepal CA-630, 150 mM NaCl) with 2-mercaptomethanol was added to the pellet, and a pipette was used to pass the lysate through it 10 times. After transferring the lysate into a sterile microcentrifuge tube, one volume of 70% ethanol was added for every volume of cell lysate and the solution was vortexed until the precipitate was dispersed. The homogenous solution was placed into a spin column with a collection tube and centrifuged at 12,000 g for 15 sec at room temperature; this was done as many times as was needed until the whole sample was centrifuged. Wash buffer I was added to the spin column and was centrifuged at 12,000 g for 15 sec at room temperature. The collection tube was discarded, and the spin column was placed in a new collection tube. Wash buffer II was added to the spin column and was then centrifuged at 12,000 g for 15 sec at room temperature. The contents of the collection tube were discarded, and the collection tube was placed back into the same collection tube; the previous step was repeated once. The spin column was centrifuged at 12,000 g for 2 min at room temperature in order to dry the silica membrane containing the now captured RNA. The spin column was then placed into a sterile microcentrifuge tube, and RNase-free water was added to the spin column, centrifuged at

12,000 g for 2 min at room temperature to elute the RNA from the silica membrane. The RNA concentration was measured using the same NanoDrop 2000 as for the DNA concentration. Once all samples' RNA concentration was measured, they were converted to cDNA.

RNA to cDNA Conversion and Polymerase Chain Reaction

To convert the isolated RNA to cDNA the High Capacity RNA-to-cDNA Kit (ThermoFisher) was used. Sterile tubes were labeled for each sample of RNA to be converted. Each tube was prepared by adding 2x RT Buffer Mix, 20x RT Enzyme Mix, the respective RNA sample, and nuclease-free water. The samples were placed into a thermal cycler at 37°C for 1hr, followed by 95°C for 5 min, and was then held at 4°C.

The newly converted cDNA samples were then amplified using the 2x PCR Taq Plus MasterMix (ABM). cDNA was amplified using the respective primers for SNAP25 and STX1A (IDT; Table 2). Each tube consisted of the converted cDNA sample, forward and reverse primers, 2x PCR Taq Plus MasterMix and nuclease-free water. The samples were denatured at 95°C for 30 sec, annealed at different temperatures for SNAP25 and STX1A, 67°C and 59.1°C respectively, extended at 72°C for 7 min, and then held at 4°C. The samples were then used for gel electrophoresis.

The gel was prepared by combining agarose (FroggaBio) and 0.5x TAE (Tris base, acetic acid glacial, 0.5 mM EDTA pH 8.0) into a glass flask and lightly cover the top so that it does not evaporate. The solution was microwaved in 20 sec increments until all the agarose was dissolved. The gel tray was prepared by placing it into a holder and inserting a 12-well comb into the top. After allowing the solution to cool down for 5min, RedSafe Nucleic Acid Staining Solution was added, and the flask was gently swirled, before pouring it into the plastic holder

mounted with the comb. While the gel was solidifying, 6x loading dye was added to each of the samples. Once the gel solidified, 100 bp DNA ladder was added, along with all the samples. The gel ran at 100 V for approximately 30 min after which it was visualized using the AlphaImager HP System (ProteinSimple; Zoidl Lab, York University).

Table 2: DNA primer forward and reverse sequences for SNAP25 and STX1A, their application in the experiments and their size.

Gene	Primer Name	Primer Sequence (5'-3')	Application	Primer Size
SNAP25	SNAP25F	TGATGAGTCCCTGGAAAGCAC	cDNA amplification	21 bp
	SNAP25R	CATCCACCACACGGGCA		17 bp
STX1A	STX1AF	GGATCATCATGGACTCCAGC	cDNA amplification	20 bp
	STX1AR	TATCCAAAGATGCCCCCGA		19 bp

Cell Transfection

Transfection was performed to introduce the purified plasmids into H9c2 and INS-1 832/13 cells using Lipofectamine 3000 (Invitrogen). This allows the DNA to enter the cells via liposomes that fuse with the cell membrane and allow them to release their contents into the cell. First, cells were split into 6-well or 12-well plates and left to adhere overnight. The following day, under sterile conditions, 24 microcentrifuge tubes were labeled, two for each construct. The tubes were aligned in two rows, such that there were 12 tubes per row. The first row contained Opti-MEM media and Lipofectamine 3000 reagent. The protocol provided instructions for two different concentrations of Lipofectamine 3000 to add to the solution, and for the purposes of this experiment, the second, or higher concentration was use as H9c2 cells tend to be quite resilient. The second row of tubes contained Opti-MEM media, P3000 reagent, the respective SNAP25 (-1517, -292, -102, -41, +22, +114) or STX1A (-1931, -1239, -627, -204, -172, -88) constructs, Renilla plasmid as internal control. The tubes were left to incubate at room temperature for 5 min, after which the tubes were combined for a total of 12 tubes, one for each construct. The wells of the plates were gently rinsed with Opti-MEM media, and a final volume of Opti-MEM was added. The tubes' contents were then dispensed into their respective wells such that the Opti-MEM/Lipofectamine solution was present in all wells. The plates were placed in the 37°C CO_2 incubator overnight. The following day, the Opti-MEM/Lipofectamine solution was removed, and regular media was added to the wells. At this point H9c2 cells were given a treatment of either TSA, FOR, or no treatment at all. The cells were incubated once more overnight, and the next day they were lysed for use in a luciferase assay. The lysis protocol for luciferase measurements is different than the one previously mentioned and will therefore be covered in the Luciferase Assay section.

Luciferase Assay and Promoter Activity

Following the full length of the transfection protocol, cells were removed from the incubator and kept on ice at non-sterile conditions. The media was removed, and the wells were gently rinsed with cold PBS two times. A 1:2 dilution was performed on the passive lysis buffer included with the Pierce Renilla/Firefly Luciferase Glow Assay Kits (ThermoFisher) and was then added to each well of the 12- or 24-well plate. The plates were placed on an orbital shaker at room temperature for 15 min. until the cells were completely lysed. The lysates were kept on the plates and placed in the freezer at -30°C while preparing the luciferase reagents. For the Renilla luciferase reagent, 100x Coloenterazine was added to the Renilla Glow Assay Buffer, and for the firefly luciferase reagent, D-Luciferin was added to the Firefly Glow Assay Buffer. The lysates were removed from the freezer and pipetted onto 96-well opaque plates (MilliporeSigma). Each sample was pipetted twice since the reading can only be obtained once for either firefly or renilla. The prepared reagents were pipetted on top of the sample and incubated at room temperature for 15 min., after which luciferase activity was measured using the Varioskan Lux luminometer (Sater Lab, York University; ThermoFisher). The luminometer was left at rest with the sample inserted for 30 seconds before commencing measurement, to reduce light bleeding, and to allow signal stabilization in the wells. The luciferase activity was then recorded from left to right starting with the upper-left most well, followed by the second row, third row, fourth row and so on, and no filters were used for measuring the wavelengths of the samples. The first and third row contained lysed samples with firefly luciferase substrate, while the second and fourth rows contained lysed samples with renilla luciferase substrate as the internal control. The luminometer generated a spreadsheet with raw luminance values for both firefly and renilla luciferase and were then exported to Microsoft Excel for further analysis. The firefly luciferase

values on the first row were divided by the renilla values in the second row, and the values in the third row were divided by the renilla luciferase values in the fourth row, in order to normalize the data to the internal renilla control.

Statistical Analysis

Data was initially recorded into a spreadsheet from the various instruments used, and were then exported to Microsoft Excel 2019, where preliminary tabulations and graphing was done. As Excel's functionality is quite limited, data were then tabulated, graphed and analyzed using GraphPad Prism (version 8.0.2). Data were separated by the two SNARE proteins, SNAP25 and STX1A, and by their respective full-length and truncated constructs. To assess the potency of TSA and FOR drug treatments on the luciferase activity, data were analyzed using a two-way analysis of variance (ANOVA) to determine which drug affected the CPR of the two SNARE proteins to a greater extent, compared to untreated (control) H9c2 cells. Post-hoc comparisons tests (Uncorrected Fisher's LSD) were performed after the ANOVA to determine the significance between untreated H9c2 cells and TSA-treated H9c2 cells, untreated H9c2 cells and FOR-treated H9c2 cells, as well as the two drug treatments themselves, TSA-treated H9c2 cells and FOR-treated H9c2 cells.

Western blotting images were imported and quantified using Image Studio Lite (version 5.2). After bands were quantified using the software, numerical values were exported, analyzed and tabulated using Microsoft Excel 2019, and densitometry graphs were obtained using the same software as for luciferase analysis. For densitometry analysis, a one-way ANOVA was performed to assess the increase of both MyoG and cTnT relative to untreated H9c2 cells, and

whether that increase was significant. In order to assess the significance of the protein increase, a Dunnett's multiple comparisons post-hoc test was performed on the densitometry data.

Results

Luciferase Reporter Activity

The data obtained from the luciferase assays were separated by the two proteins of interest, SNAP25 and STX1A. Luciferase activity was initially assessed in INS-1 832/13 cells to obtain baseline measurements for the transfected constructs. Data were plotted as relative luminometer units (RLU) for each construct and values were calculated by dividing the absorbance values recorded from firefly luciferase by the absorbance of Renilla luciferase, since Renilla was the internal control. The highest luciferase activity was noted to be in the CPR, at the -292 and -102 for SNAP25 (Figure 9), and the CPR of STX1A, at -204 (Figure 10) which corresponds to the findings of Shimada et al. (2007) and Nakayama et al. (2016) in granulosa cells and PC12 cells, respectively, with these promoter constructs.

Following transfection using the pGL3 vector containing truncated regions of the upstream promoter, H9c2 cells were treated with either TSA, FOR, or not treated at all. Shimada and colleagues (2007) demonstrated FOR significantly enhanced SNAP25 reporter activity. Similarly, Nakayama et al. (2016, 2017) showed either TSA or FOR could increase STX1A reporter activity in skin keratinocyte FRSK cells and fibroblasts. Their experiments were repeated in this study to determine if a similar regulatory response of the SNAP25 and STX1A reporter could be observed in H9c2 cells. The luciferase reporter assay results can be seen in figures 11 and 12 for SNAP25 and STX1A, respectively. A two-way ANOVA was performed to analyze the effects of TSA and FOR against untreated H9c2 cells, as well as the potency of the two drugs relative to each other. A two-way analysis of variance was conducted on two independent variables for SNAP25 (constructs and treatments) which yielded a main effect of $F(2,54) = 57.64$, $p < .0001$ and an interaction effect of $F(10,54) = 7.51$, $p < .0001$, and as such

they are both considered extremely significant. A significant increase was noted with the -292 transfected region between control H9c2 cells (17.5 ± 0.9) and cells treated with either TSA (25.3 ± 1.0) or FOR (20.6 ± 0.6). It is also worth noting that there was a significant difference noted between the two treatments groups ($p < 0.001$). There was a marked increase in luciferase activity via TSA treatment compared to FOR, although both showed a significant increase relative to untreated H9c2. Although the CPR of the SNARE proteins showed significant differences across treatments, some of the flanking regions also showed significant differences.

At the most upstream position, there was a significant difference for the -1517 construct between untreated H9c2 (17.5 ± 0.9) and the TSA treatment (25.3 ± 1.0) ($p < 0.001$) as well as TSA (25.3 ± 1.0) and FOR (20.6 ± 0.6) ($p < 0.001$), but there was no significant difference between untreated H9c2 and FOR. Moving downstream on the promoter past the CPR, the -102 and -41 constructs showed some significant differences. For -102 there was significant differences between untreated H9c2 (17.5 ± 0.9) and TSA (25.3 ± 1.0), untreated H9c2 and FOR (20.6 ± 0.6), as well as TSA and FOR ($p < 0.001$). For the -41 construct, significant differences were noted between untreated H9c2 (17.5 ± 0.9) and TSA (25.3 ± 1.0) as well as the two treatments themselves, TSA and FOR (20.6 ± 0.6) ($p < 0.001$), but no significant difference was noted between untreated H9c2 and FOR. At the last two downstream constructs, +22 and +114, there were no significant differences noted between either untreated H9c2 and the two drug treatments, nor between TSA and FOR.

In the case of STX1A constructs, similar patterns were noted as with the SNAP25 CPR region. Maintaining the same independent variables, a two-way analysis of variance (ANOVA) was conducted, which yielded a main effect of $F(2,54) = 88.69$, $p < .0001$ and an interaction effect of $F(10,54) = 5.749$, $p < .0001$, and similarly to the SNAP25 promoter analysis, they are

both considered extremely significant. A significant increase in the RLU was noted with the -204 transfected region between untreated H9c2 (19.4 ± 0.6) and TSA (27.0 ± 1.0) ($p < 0.001$). Similarly, a significant difference was noted between untreated H9c2 and FOR (23.9 ± 1.0) ($p < 0.001$), as well, a significant difference between the two drug treatments is observed, which goes to show that TSA had a significant increase relative to FOR ($p = 0.002$). Although TSA had a greater effect on luciferase activity than FOR, a greater increase on luciferase activity was noted from both drug treatments relative to untreated H9c2 cells.

There were some significant differences noted upstream and downstream of the CPR. At the most upstream end of the promoter, the full-length -1931 construct showed significant differences between control H9c2 (19.4 ± 0.6) and TSA treatment (27.0 ± 1.0) ($p = 0.005$), as well as control H9c2 and the FOR treatment (23.9 ± 1.0) ($p < 0.01$), but there was no significant difference noted between the two treatment conditions TSA and FOR as was otherwise noted in the CPR. Moving further down, the -1239 construct showed significant differences between control/untreated H9c2 (19.4 ± 0.6) and TSA (27.0 ± 1.0) ($p < 0.001$), as well as control H9c2 and FOR (23.9 ± 1.0) ($p = 0.003$), however, no significant difference was noted between the two drug treatments, TSA and FOR. Directly flanking the CPR upstream, the -627 construct showed significant differences between untreated H9c2 (19.4 ± 0.6) and TSA (27.0 ± 1.0) ($p < 0.001$), untreated H9c2 and FOR (23.9 ± 1.0) ($p = 0.024$), and TSA and FOR ($p < 0.001$). Downstream of the CPR, the -172 region, similarly to the -627 construct, showed significant differences between untreated H9c2 (19.4 ± 0.6) and TSA (27.0 ± 1.0) ($p < 0.001$), untreated H9c2 and FOR (23.9 ± 1.0) ($p < 0.001$), and TSA and FOR ($p < 0.001$). At the most downstream end of the gene, the -88 promoter construct showed a significant difference only between the two drug

treatments TSA (27.0 ± 1.0) and FOR (23.9 ± 1.0) ($p = 0.017$), and no significant difference between untreated H9c2 cells and either of the drug treatments, TSA and FOR.

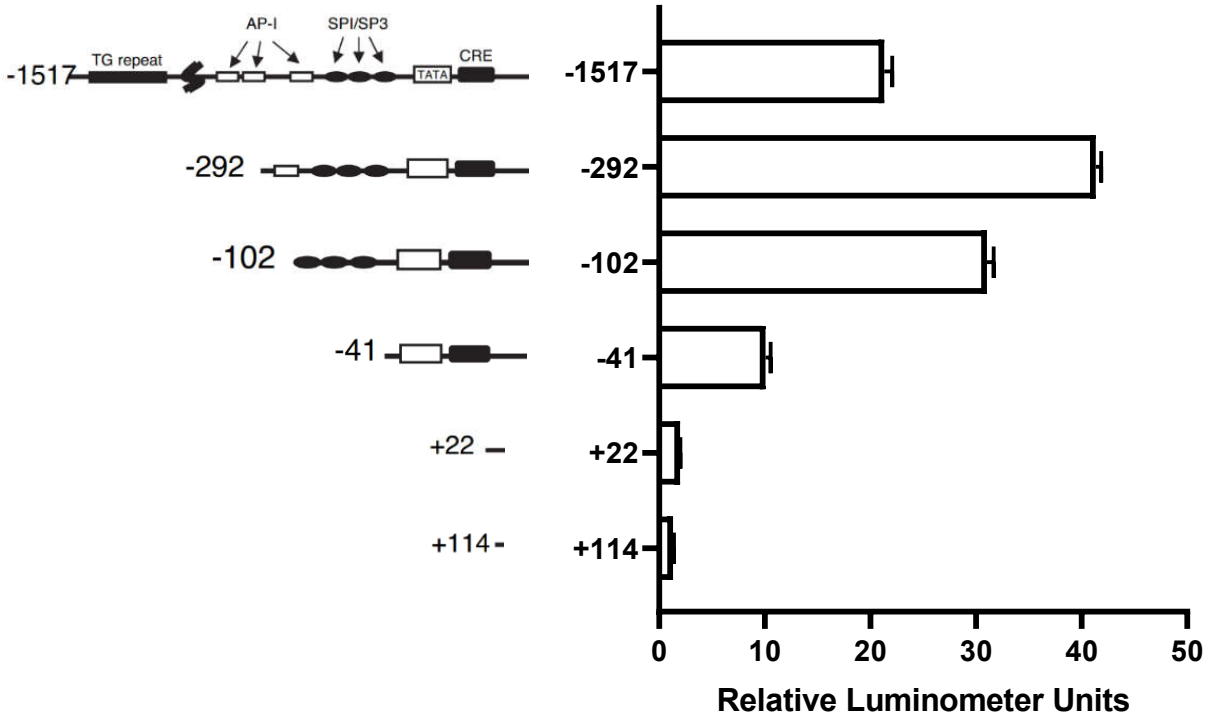

Figure 9: SNAP25 promoter activity in INS-1 832/13 cells transfected with the full-length or truncated regions of the SNAP25 promoter. The -292 and -102 bp promoters had the highest activity which has been reported to be the core promoter region for SNAP25 (Shimada et al., 2007). Data represent means ± SEM from 4 separate experiments.

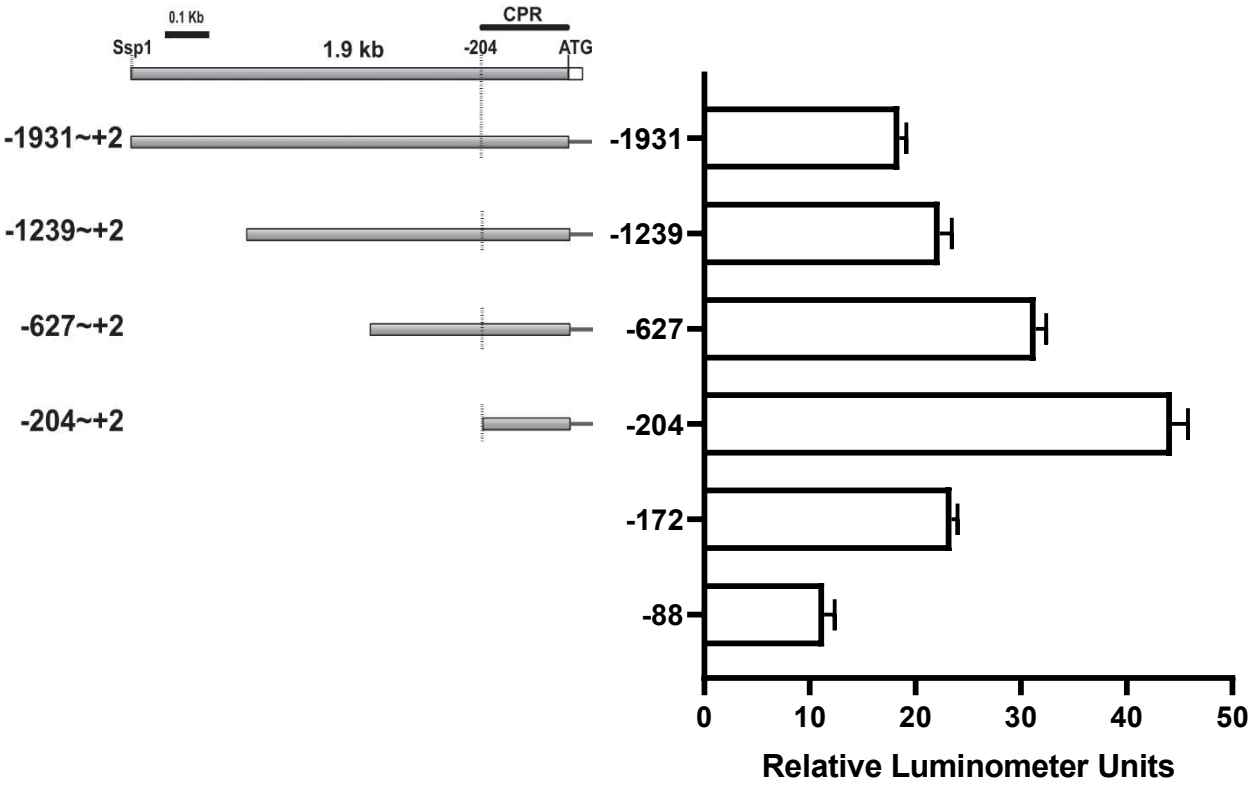

Figure 10: STX1A promoter activity in INS-1 832/13 cells. Cells were transfected with full-length or truncated regions of the upstream promoter of STX1A. The -204 bp STX1A promoter had the greatest activity which was demonstrated by Nakayama et al. (2016) to be the core promoter region. Data represent means ± SEM (n=4).

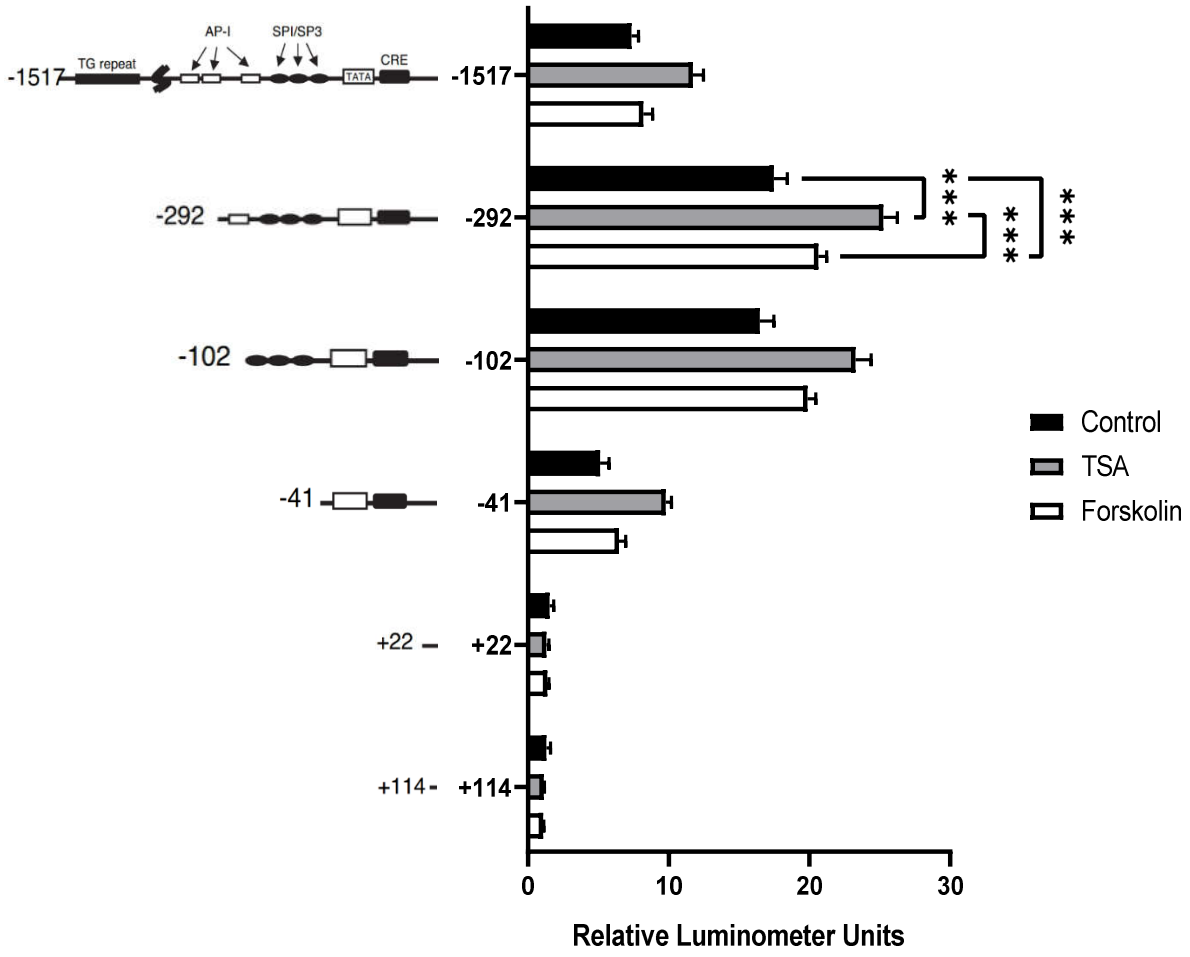

Figure 11: SNAP25 promoter activity in H9c2 cells. Full-length or truncated regions of the upstream promoter regions of SNAP25 were transfected into H9c2 cells. H9c2 cells were also treated with either TSA or forskolin. The left side of the graph represents clipped constructs from Shimada and colleagues (2007). Untreated H9c2 cells are represented by the black bars, H9c2 cells treated with trichostatin A (TSA) in grey, and forskolin treated H9c2 cells in white. Data represent means ± SEM from 4 separate experiments.

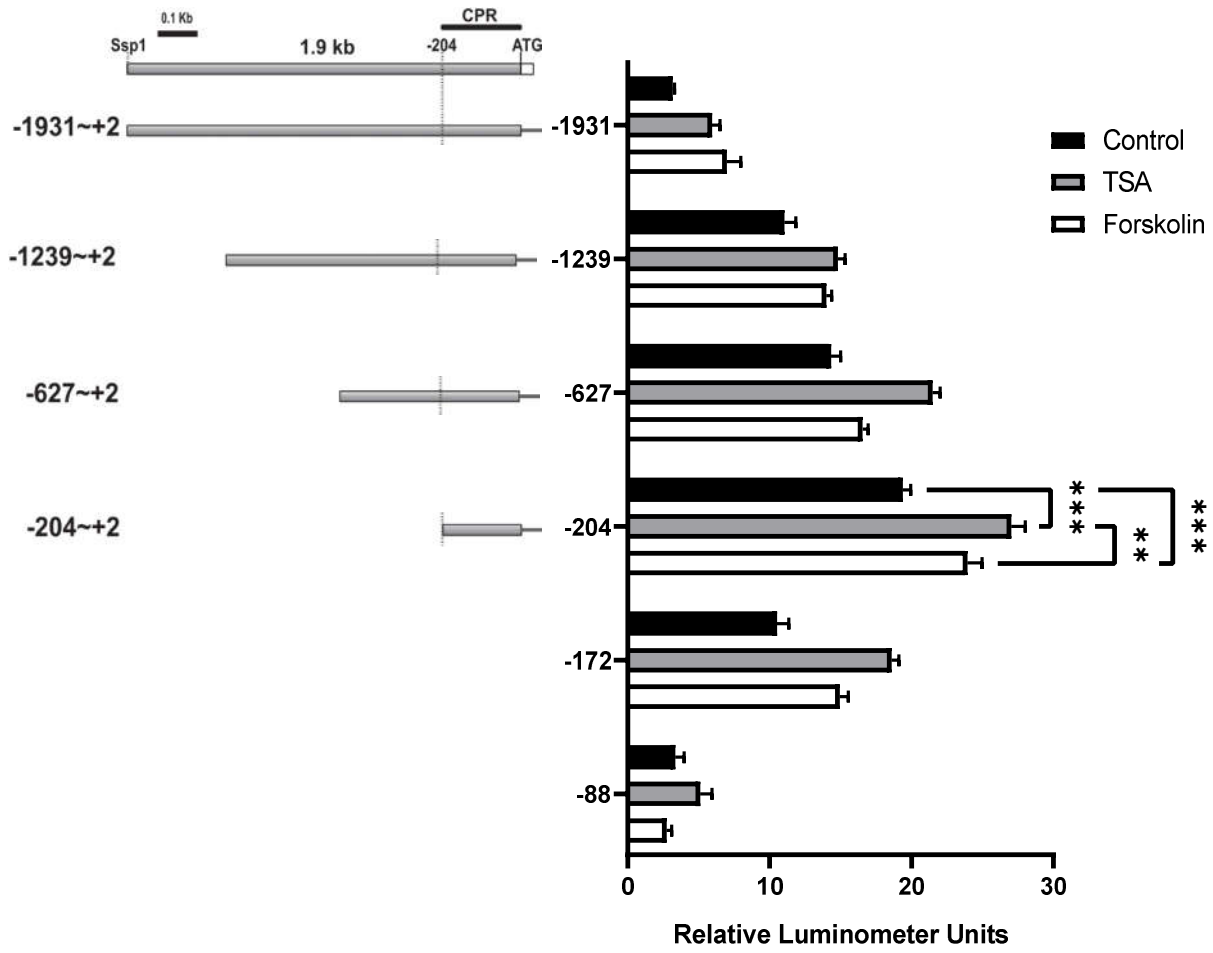

Figure 12: STX1A promoter activity of full-length or truncated regions transfected into H9c2 cells. H9c2 cells were treated with either TSA or forskolin. The left side of the graph represents clipped constructs from Nakayama and colleagues' (2016). Untreated H9c2 cells are represented by the black bars, H9c2 cells treated with trichostatin A (TSA) in grey, and forskolin treated H9c2 cells in white. Data represent means ± SEM (n=4).

Western Blotting Analysis

H9c2 cells were treated with TSA, FOR, RA, or transfected with a pCMV vector containing Sp1 sites. Nakayama and colleagues (2016, 2017) demonstrated STX1A protein expression could be induced in FRSK skin keratinocyte cells and fibroblasts, which do not endogenously express this SNARE protein, following treatment with TSA, FOR or ectopic expression of Sp1. Membranes were blotted for the SNARE proteins, SNAP25 and STX1A, as well as markers for cardiac and skeletal muscle differentiation cTnT, and MyoG, respectively (Figure 13). No bands were detected for either SNAP25 or STX1A in treated H9c2 cells. The H9c2 lysates were also blotted for cardiac and skeletal markers, and it can be seen in figure 13 that both cTnT and MyoG expression was enhanced via all treatments, TSA, FOR, 3-day and 7-day treatments. Western blots were repeated for cTnT and MyoG in order to perform densitometry analyses (Figure 14 and 15). An analysis of variance showed that the effects of drug treatments and differentiation protocols on inducing cTnT expression were significant, $F(4,10) = 12.99$, $p < .001$. Post hoc analyses using Dunnett's multiple comparisons test showed a relatively higher protein expression across the board from for TSA (3.2 ± 0.3), FOR (3.7 ± 0.3), 3-day RA treatment (4.1 ± 0.5), and 7-day RA treatment (2.7 ± 0.3) relative to control.

A similar analysis of variance on the induction of MyoG via drug and differentiation treatments showed that MyoG protein expression was significant, $F(4,10) = 31.17$, $p < .0001$; TSA (3.1 ± 0.3), FOR (3.1 ± 0.5), 3-day RA treatment (5.4 ± 0.5) and 7-day RA treatment (8.3 ± 0.8). All showed a significant increase in both cardiac and skeletal muscle biomarkers, with a marked tendency towards the latter, which is not the expected result. The hypothesis is partially true, as although there was an increase in both cardiac and skeletal muscle markers, the goal was to shift H9c2 cells towards a more cardiac type, while at the same time, reducing skeletal muscle

biomarkers. The null hypothesis is then accepted, as H9c2 tended towards a more skeletal muscle type, rather than cardiac.

Furthermore, H9c2 cells were also transfected with a pCMV vector containing Sp1 gene but this also failed to induce SNARE expression in H9c2 cells (Figure 16). No bands were observed for either SNAP25 or STX1A, across the three replicates transfected with Sp1-containng pCMV vector. The only bands observed were the positive brain control for both SNAP25 and STX1A, and the GAPDH loading control.

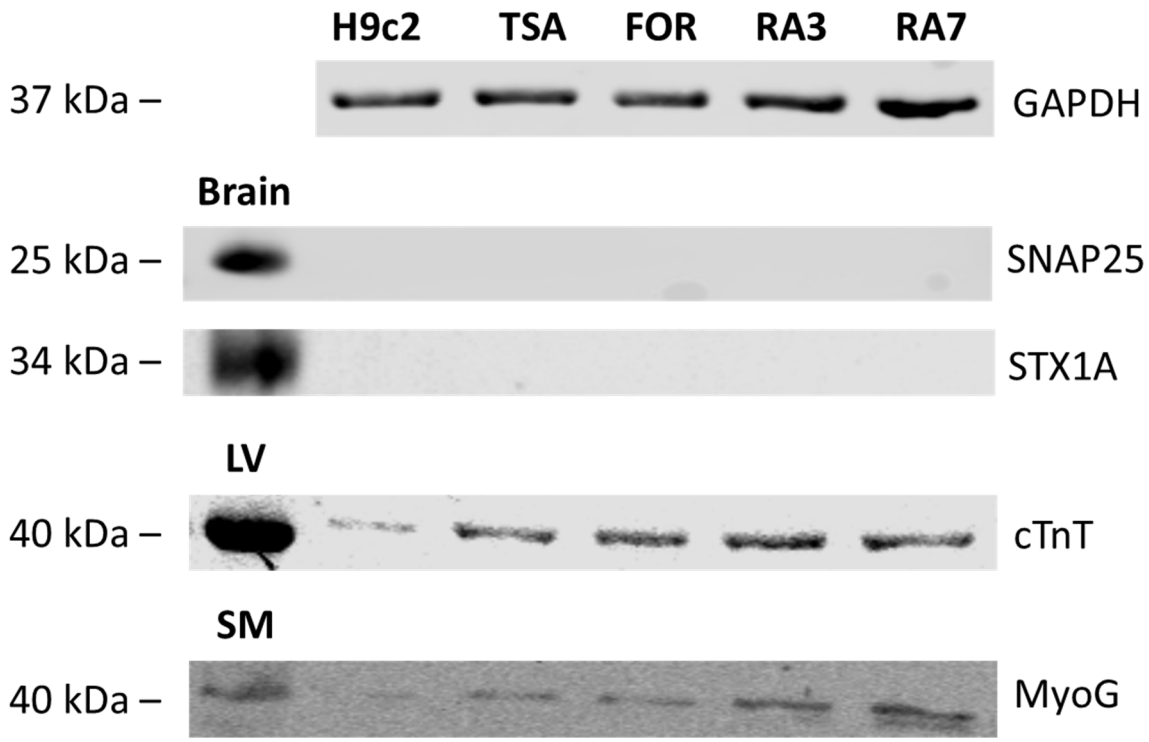

Figure 13: Western blotting of SNARE proteins, as well as cardiac and skeletal markers. Brain sample was used as positive control for SNAP25 and STX1A, left ventricle (LV) was used as positive control for cTnT, and skeletal muscle (SM) was used as positive control for MyoG. All positive control samples were obtained from mouse. Samples loaded in wells correspond (from left to right) with untreated H9c2 cells (H9c2), TSA treated H9c2 cells (TSA), forskolin treated H9c2 cells (FOR), and H9c2 cells treated with retinoic acid for 3 days (RA3) and 7 days (RA7). No SNAP25 and STX1A expression was observed in any of the treatment conditions. Cardiac and skeletal markers were found to be expressed in H9c2 cells in the form of cTnT and myogenin, respectively, for all treatment conditions.

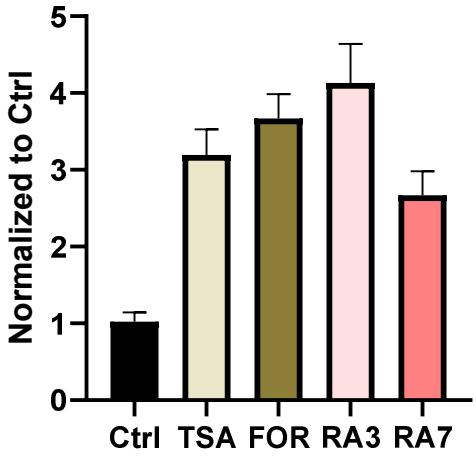

Figure 14: Densitometry was performed on the cTnT blots (normalized to GAPDH). Samples correspond (from left to right) with untreated H9c2 cells (Ctrl), TSA treated H9c2 cells (TSA), forskolin treated H9c2 cells (FOR), and H9c2 cells treated with retinoic acid for 3 days (RA3) and 7 days (RA7). There was an increase noted in all treatment conditions relative to untreated H9c2 cells. There is a drop in cTnT expression in the 7-day RA treatment relative to the 3-day RA treatment. Data represent means ± SEM.

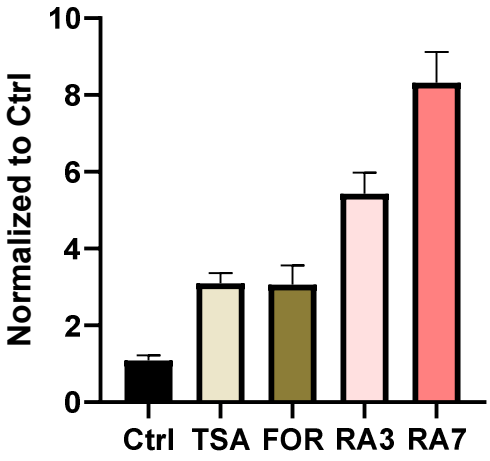

Figure 15: Densitometry was performed on the MyoG blots (normalized to GAPDH). Samples correspond (from left to right) with untreated H9c2 cells (Ctrl), TSA treated H9c2 cells (TSA), forskolin treated H9c2 cells (FOR), and H9c2 cells treated with retinoic acid for 3 days (RA3) and 7 days (RA7). There was an increase noted in all treatment conditions relative to untreated H9c2 cells. A marked increase is noted in the RA treatments compared to the TSA and FOR treatments. Data represent means ± SEM.

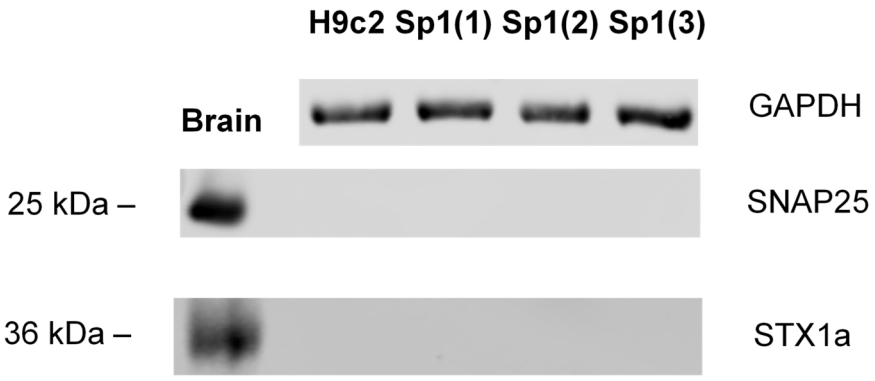

Figure 16: Western blotting of SNARE proteins, following transfection of three different H9c2 batches. Positive control in the first well is a brain sample obtained from mouse. From left to right, the protein samples correspond to untreated H9c2 cells (H9c2), and three separately transfected H9c2 batches with pCMV plasmid containing Sp1 (Sp1(1), Sp1(2), Sp1(3)). No SNAP25 or STX1A was observed in any of the three repeats of pCMV Sp1 transfected H9c2 plates. Present bands are brain positive control and GAPDH was used as a loading control.

PCR and DNA electrophoresis

Since Western blotting did not detect SNARE expression in H9c2 cells, it was prudent to check whether the message for SNAP25 and STX1A transcripts were present. For PCR analysis, cells were treated with TSA, or FOR (Figure 16). H9c2 cells have also been transfected with a pCMV vector containing Sp1 sites and RNA has been isolated in order to observe if the presence of Sp1 sites alters the expression of SNAP25 and STX1A. INS-1 832/13 cDNA was used as a positive control for both PCR gels, as these cells endogenously express SNAP25 and STX1A; INS-1 832/13 cell PCR reactions were optimized for their respective annealing temperatures for each of the SNARE proteins. Results for the PCR gel electrophoresis were not conclusive and as such, they were excluded from the results and no analysis was performed.

Discussion

The goal of this study was to assess the regulatory mechanisms of SNAP25 and STX1A gene promoters in a cardiac cell model. For this study, the INS-1 832/13 cell line was also selected due to their ability to endogenously express SNAP25 and STX1A for the purposes of comparison to H9c2 cells (Hectors et al., 2013; Salunkhe et al., 2017). H9c2 cells were also used as a cardiac model due to their origin being from neonatal ventricular mouse tissue, with the expectation that they would mimic development of a neonatal cardiac model to adulthood. The goal was to determine if SNARE expression could be induced via epigenetic means as per other studies (Nakayama & Akagawa, 2017; Nakayama et al., 2016; Shimada et al., 2007), and to examine the regulatory mechanisms underlying their expression in a developing cardiac model.

The present study also wanted to confirm the core promoter regions to be the same as those found in the literature by Nakayama and Shimada for SNAP25 and STX1A (Nakayama et al., 2016; Shimada et al., 2007), which it was able to confirm. The hypothesis for this study was that treating the cells with TSA and FOR would induce SNARE expression, and that differentiation of H9c2 cells via RA would take them towards a more cardiac phenotype and less of a skeletal muscle one. However, Western blotting showed SNARE expression was not inducible in H9c2 cells via any of the drug treatments, including the differentiation protocol with RA and reduced serum FBS as per other studies which have been successful in doing so (Branco et al., 2015; Kaneda et al., 2005; Menard et al., 1999; Ruiz et al., 2012; Sucharov et al., 2006). Furthermore, the hypothesis that H9c2 cells' differentiation will tend them to a more cardiac phenotype is also partially confirmed. The cells did exhibit some cardiac markers as evidenced by Western blotting and densitometry analysis, but the same analysis also showed that H9c2

cells tended to differentiate towards a more skeletal muscle phenotype and less of a cardiac one (Figures 7 and 15).

Luciferase Analysis

Luciferase assays were performed in order to ascertain the SNAP25 and STX1A promoter activity profile and to determine if the CPR was in the same upstream region as those regions found by Shimada and colleagues (2007) for SNAP25 and Nakayama and colleagues (2016) for STX1A (Figures 9-12). The SNAP25 CPR was shown to be -292→-102 and activity appeared to drop upstream and downstream of that CPR, lending validity to the presence of repressor genes upstream, and to the integral part of Sp1 sites contained within the -292→-102 region as an important region for epigenetic regulation (Nakayama et al., 2016; Ryabinin et al., 1995; Sucharov et al., 2006; Waby et al., 2008). The STX1A CPR was shown to be from -204→+2 as per previous studies, showing that repressor genes upstream of that inhibit the expression of STX1A.

In the case of SNAP25, -292 was not the only construct found to have significant differences across treatments. The most upstream region, -1517, showed significant differences between control H9c2 and TSA treated cells, as well as TSA and FOR. Downstream from the CPR, the -102 construct showed a significant difference across all three comparisons, control H9c2 and TSA, control H9c2 and FOR, and TSA and FOR. Since this area is quite close to the CPR, most of the key enhancer elements are still found in this sequence, which could explain why significant differences were found across all conditions. The last SNAP25 construct to show any significant difference was -41, for untreated H9c2 and TSA, and TSA and FOR. Neither +22 nor +114 showed any significant difference between any of the treatment conditions. That is in

part to be expected as they are the most distal regions from the CPR and do not contain the key binding sites that -292 does, including, but not limited to, the Sp1 sites.

For STX1A, although the greatest promoter activity and significant differences were found in the -204+2 region, some of the flanking regions had some notable statistical differences as well. Starting with the most upstream region, -1931 showed significant differences between untreated H9c2 and TSA, as well as untreated H9c2 and FOR. The same significant differences are found in the immediate flanking region downstream of -1931, at -1239. These differences show TSA being a potent epigenetic regulator even when repressor elements are present, if the CPR is contained within the gene. The -627 construct showed significant differences between all three treatment conditions, like the CPR of -204. Most of the same required regions are most likely to be found in the both constructs with only some repressor sequences present.

TSA seemed to have had a greater effect on untreated H9c2 as opposed to FOR, and TSA also showed a higher increase relative to FOR, marking it as a more potent epigenetic regulator than FOR, at the very least in the case of H9c2 and the scope of this study. The last construct to show significant differences was -172, with -88 only showing a notable difference between the two drug treatments TSA and FOR, and so no conclusions can be made with relation to untreated cells at that construct. At -172, however, all three groups showed significant differences compared to each other similarly to -204. Being only 32 base pairs away from each other, it is no surprise that -172 would contain many of the same enhancer and critical regions that -204 would contain.

The baseline promoter activity in INS-1 832/13 for both SNAP25 and STX1A for all constructs can be seen in figures 9 and 10. This activity is then found to be quite a magnitude higher than in H9c2 cells (Figures 11 and 12); in fact, it is almost double for both SNAP25 and

STX1A (Salunkhe et al., 2017). That is of course to be expected as H9c2 cells were only transiently expressing SNAP25 and STX1A post-transfection of the upstream promoter sites. With a cell line that endogenously expresses these two SNARE proteins, it was expected that the promoter activity would have been higher for INS-1 832/13 cells. The lower activity could have been due to signal degradation between adding the luciferase substrate and measurement of the signal itself, as external light, although kept to a minimum, can degrade the luciferase and Renilla substrates.

Further assessment of the regulation of SNAP25 and STX1A promoter activity in H9c2 cells was done by implementing the treatments of an HDAC inhibitor and a PKA activator. TSA has been found to be a potent HDAC inhibitor, and studies have reported higher levels of histone acetylation due to TSA activity influencing gene expression (Yoshida & Horinouchi, 1999). Along those lines, Nakayama and colleagues (2016) were able to show the induction of STX1A mRNA expression via TSA treatment. In tandem, FOR, a PKA activator, was applied as it is known to potently induce expression of other genes (Hernandez-Gonzalez et al., 2006; Sriraman, Rudd, Lohmann, Mulders, & Richards, 2006).

Figures 11 and 12 however also show that H9c2 SNARE transcriptional activity can be altered via epigenetic means, as has also been done previously (Hescheler et al., 1991; Shimada et al., 2007; Whittle & Singewald, 2014). The ANOVA performed revealed a significant difference between groups, from H9c2 to TSA, H9c2 to FOR, and even TSA to FOR. The latter revealed that TSA is in fact a more potent epigenetic regulator via its HDAC inhibition than the FOR treatment and its CREB pathway. A more relaxed chromatin seems to be the key to transcriptional activation of SNAREs as opposed to the CREB pathway (Branco et al., 2015; Kaneda et al., 2005).

Protein Expression and Densitometry

Western blotting was unable to detect SNARE protein expression of STX1A or SNAP25 in H9c2 cells (Figure 13). This was attempted via TSA or FOR treatments, differentiation using RA for 3 and 7 days, and via transfection with a pCMV vector for the transient expression of Sp1 plasmid DNA in H9c2 cells. Since none of the treatments were able to induce SNARE expression, the hypothesis is therefore rejected.

H9c2 cells were also blotted for cardiac or skeletal markers, as they are known to be multipotent, and being derived from embryonic ventricular tissue, they have the potential to develop into both cardiac tissue, as well as skeletal muscle (Branco et al., 2015; Kaneda et al., 2005; Kimes & Brandt, 1976; Ruiz et al., 2012). Cardiac and skeletal markers were indeed found across all treatments, even with some faint bands present under the H9c2 control (Figure 13). The experiment was this successful in the differentiation of H9c2 cells into both a cardiac and skeletal muscle type. However, when performing densitometry analysis on the blots themselves, something less than ideal was noted. Figures 14 and 15 indicate that H9c2 cells steered towards a both a cardiac and skeletal muscle type, as evidenced by the increase in cTnT and myogenin, respectively.

The goal of this study was to look at SNARE expression in a cardiac model, and differentiation of these cells in fact caused them to become more skeletal muscle-like. A cardiac marker increase can be noted across all treatments with the peak occurring at the 3-day RA treatment, and then dropping for the 7-day treatment, indicating that longer RA treatments will not necessarily induce differentiation towards a more cardiac phenotype. The 3 and 7-day RA treatment lead to an increase in MyoG to a higher extent than it did the increase in cTnT. This goes against previous research which has shown that H9c2 cells tend to a more cardiac

phenotype following RA treatment, as well as a reduction in skeletal muscle markers (Branco et al., 2015; Menard et al., 1999; Pereira et al., 2011). That is not to say that it was unlikely, as H9c2 cells are multipotent, with the ability to differentiate into skeletal muscle cells, but previous research had found the presence of skeletal muscle markers to reduce in favor of more cardiac markers.

Conclusions

The findings of this study have several implications outside of the lab environment. Although to a lesser extent than skeletal muscle, the cells' ability to differentiate towards a cardiac marker is a promising reinforcement that H9c2 cells can be used in place of live mice for cardiac research. The cells' ability to differentiate into either cardiac or skeletal muscle cells, allows for more niche research questions to be asked, such as cross-correlational studies that look at both cardiac and skeletal muscle markers. Luciferase assays were able to confirm previous literature, and further work on the promoter regions of SNAP25 and STX1A might shed more light onto their underlying mechanisms. More specifically, closer attention to the Sp1/Sp3 sites as enhancer regions, as well as the AP-1 site which might function as a gene repressor. A co-transfection of Sp1/Sp3 along with the truncated promoter regions of SNAP25 and STX1A, might yield a more robust representation of the gene promoters of these two proteins and the effect Sp1 sites have on their epigenetic regulation.

Most importantly, a limitation of this study stems from using the H9c2 cell line. Although they are a cell line that can be employed in various scenarios, due to their multipotent nature, ultimately, they are not true cardiac cells. Employing some of the same experimental procedures outlined in this study, but in neonatal cardiomyocytes might be the answer to observing SNARE expression during cardiac development.

References

Branco, A. F., Pereira, S. P., Gonzalez, S., Gusev, O., Rizvanov, A. A., & Oliveira, P. J. (2015). Gene expression profiling of H9c2 myoblast differentiation towards a cardiac-like phenotype. *PLoS ONE*, *10*(6), 1–18. https://doi.org/10.1371/journal.pone.0129303

Brophy, K., Hawi, Z., Kirley, A., Fitzgerald, M., & Gill, M. (2002). Synaptosomal-associated protein 25 (SNAP-25) and attention deficit hyperactivity disorder (ADHD): Evidence of linkage and association in the Irish population. *Molecular Psychiatry*, *7*(8), 913–917. https://doi.org/10.1038/sj.mp.4001092

Burns, W. R., & Edil, B. H. (2012). Neuroendocrine pancreatic tumors: Guidelines for management and update. *Current Treatment Options in Oncology*. https://doi.org/10.1007/s11864-011-0172-2

Burri, L., & Lithgow, T. (2004). A complete set of SNAREs in yeast. *Traffic*, *5*(1), 45–52. https://doi.org/10.1046/j.1600-0854.2003.00151.x

Cai, F., Chen, B., Zhou, W., Zis, O., Liu, S., Holt, R. A., … Song, W. (2008). SP1 regulates a human SNAP-25 gene expression. *Journal of Neurochemistry*, *105*(2), 512–523. https://doi.org/10.1111/j.1471-4159.2007.05167.x

Cauliez, B., Berthe, M. C., & Lavoinne, A. (2005). Brain natriuretic peptide: physiological, biological and clinical aspects. *Annales de Biologie Clinique*, *63*(1), 15–25. Retrieved from http://www.ncbi.nlm.nih.gov/pubmed/15689309

Chao, C. C. T., Mihic, A., Tsushima, R. G., & Gaisano, H. Y. (2011). SNARE protein regulation of cardiac potassium channels and atrial natriuretic factor secretion. *Journal of Molecular and Cellular Cardiology*, *50*(3), 401–407. https://doi.org/10.1016/j.yjmcc.2010.11.018

Chapman, E. R. (2002). Synaptotagmin: A Ca2+ sensor that triggers exocytosis? *Nature Reviews*

Molecular Cell Biology, *3*(7), 498–508. https://doi.org/10.1038/nrm855

de Bold, A J, Borenstein, H. B., Veress, A. T., & Sonnenberg, H. (1981). A rapid and potent natriuretic response to intravenous injection of atrial myocardial extract in rats. *Life Sciences*, *28*(1), 89–94. https://doi.org/10.1016/0024-3205(81)90370-2

De Bold, Adolfo J. (1985). Atrial natriuretic factor: A hormone produced by the heart. *Science*, *230*(4727), 767–770. https://doi.org/10.1126/science.2932797

Duman, J. G., & Forte, J. G. (2003). What is the role of SNARE proteins in membrane fusion? *American Journal of Physiology. Cell Physiology*, *285*(71), C237–C249. https://doi.org/10.1152/ajpcell.00091.2003

Dun, A. R., Rickman, C., & Duncan, R. R. (2010). The t-SNARE complex: A close up. In *Cellular and Molecular Neurobiology* (Vol. 30, pp. 1321–1326). https://doi.org/10.1007/s10571-010-9599-4

Dynlacht, B. D., Hoey, T., & Tjian, R. (1991). Isolation of coactivators associated with the TATA-binding protein that mediate transcriptional activation. *Cell*, *66*(3), 563–576. https://doi.org/10.1016/0092-8674(81)90019-2

Fasshauer, D., Sutton, R. B., Brunger, A. T., & Jahn, R. (1998). Conserved structural features of the synaptic fusion complex: SNARE proteins reclassified as Q- and R-SNAREs. *Proceedings of the National Academy of Sciences*, *95*(26), 15781–15786. https://doi.org/10.1073/pnas.95.26.15781

Feinshreiber, L., Singer-Lahat, D., Ashery, U., & Lotan, I. (2009). Voltage-gated potassium channel as a facilitator of exocytosis. In *Annals of the New York Academy of Sciences* (Vol. 1152, pp. 87–92). https://doi.org/10.1111/j.1749-6632.2008.03997.x

Ferlito, M., Fulton, W. B., Zauher, M. A., Marbán, E., Steenbergen, C., & Lowenstein, C. J.

(2010). VAMP-1, VAMP-2, and syntaxin-4 regulate ANP release from cardiac myocytes. *Journal of Molecular and Cellular Cardiology*, *49*(5), 791–800. https://doi.org/10.1016/j.yjmcc.2010.08.020

Florea, V. G., & Cohn, J. N. (2014, May 23). The autonomic nervous system and heart failure. *Circulation Research*. https://doi.org/10.1161/CIRCRESAHA.114.302589

Frietze, S., & Farnham, P. J. (2011). Transcription factor effector domains. *Sub-Cellular Biochemistry*, *52*, 261–277. https://doi.org/10.1007/978-90-481-9069-0_12

Galaburda, A. M., Holinger, D. P., Bellugi, U., & Sherman, G. F. (2002). Williams syndrome. Neuronal size and neuronal-packing in primary visual cortex. *Archives of Neurology*, *59*, 1461–1467. https://doi.org/10.1038/nn.4276.Neurobiology

Gao, M. C., Bellugi, U., Dai, L., Mills, D. L., Sobel, E. M., Lange, K., & Korenberg, J. R. (2010). Intelligence in williams syndrome is related to STX1A, which encodes a component of the presynaptic SNARE complex. *PLoS ONE*, *5*(4), e10292. https://doi.org/10.1371/journal.pone.0010292

Glick, B. S., & Rothman, J. E. (1987). Possible role for fatty acyl-coenzyme A in intracellular protein transport. *Nature*, *326*(6110), 309–312. https://doi.org/10.1038/326309a0

Gomez Stallons, M. V., Wirrig-Schwendeman, E. E., Fang, M., Cheek, J. D., Alfieri, C. M., Hinton, R. B., & Yutzey, K. E. (2016). Molecular Mechanisms of Heart Valve Development and Disease. In *Etiology and Morphogenesis of Congenital Heart Disease: From Gene Function and Cellular Interaction to Morphology* (pp. 145–151). https://doi.org/10.1007/978-4-431-54628-3_18

Hakami, N. Y., Dusting, G. J., & Peshavariya, H. M. (2016). Trichostatin A, a histone deacetylase inhibitor suppresses NADPH Oxidase 4-Derived Redox Signalling and

Angiogenesis. *Journal of Cellular and Molecular Medicine*, *20*(10), 1932–1944. https://doi.org/10.1111/jcmm.12885

Han, J., Pluhackova, K., & Böckmann, R. A. (2017). The multifaceted role of SNARE proteins in membrane fusion. *Frontiers in Physiology*, *8*(JAN). https://doi.org/10.3389/fphys.2017.00005

Hanft, L. M., Cornell, T. D., McDonald, C. A., Rovetto, M. J., Emter, C. A., & McDonald, K. S. (2016). Molecule specific effects of PKA-mediated phosphorylation on rat isolated heart and cardiac myofibrillar function. *Archives of Biochemistry and Biophysics*, *601*, 22–31. https://doi.org/10.1016/j.abb.2016.01.019

Hectors, T. L. M., Vanparys, C., Pereira-Fernandes, A., Martens, G. A., & Blust, R. (2013). Evaluation of the INS-1 832/13 Cell Line as a Beta-Cell Based Screening System to Assess Pollutant Effects on Beta-Cell Function. *PLoS ONE*, *8*(3), e60030. https://doi.org/10.1371/journal.pone.0060030

Hernandez-Gonzalez, I., Gonzalez-Robayna, I., Shimada, M., Wayne, C. M., Ochsner, S. A., White, L., & Richards, J. S. (2006). Gene Expression Profiles of Cumulus Cell Oocyte Complexes during Ovulation Reveal Cumulus Cells Express Neuronal and Immune-Related Genes: Does this Expand Their Role in the Ovulation Process? *Molecular Endocrinology*, *20*(6), 1300–1321. https://doi.org/10.1210/me.2005-0420

Hescheler, J., Meyer, R., Plant, S., Krautwurst, D., Rosenthal, W., & Schultz, G. (1991). Morphological, biochemical, and electrophysiological characterization of a clonal cell (H9c2) line from rat heart. *Circulation Research*, *69*(6), 1476–1486. https://doi.org/10.1161/01.RES.69.6.1476

Hohmeier, H. E., Mulder, H., Chen, G., Henkel-Rieger, R., Prentki, M., & Newgard, C. B.

(2000). Isolation of INS-1-derived cell lines with robust ATP-sensitive K+ channel-dependent and -independent glucose-stimulated insulin secretion. *Diabetes*, *49*(3), 424–430. https://doi.org/10.2337/diabetes.49.3.424

Hong, W. (2005). SNAREs and traffic. *Biochimica et Biophysica Acta - Molecular Cell Research*. https://doi.org/10.1016/j.bbamcr.2005.03.014

Hu, K., Carroll, J., Rickman, C., & Davletov, B. (2002). Action of complexin on SNARE complex. *Journal of Biological Chemistry*, *277*(44), 41652–41656. https://doi.org/10.1074/jbc.M205044200

Iezzi, S., Di Padova, M., Serra, C., Caretti, G., Simone, C., Maklan, E., … Sartorelli, V. (2004). Deacetylase inhibitors increase muscle cell size by promoting myoblast recruitment and fusion through induction of follistatin. *Developmental Cell*, *6*(5), 673–684. https://doi.org/10.1016/S1534-5807(04)00107-8

Jeans, A. F., Oliver, P. L., Johnson, R., Capogna, M., Vikman, J., Molnár, Z., … Davies, K. E. (2007). A dominant mutation in Snap25 causes impaired vesicle trafficking, sensorimotor gating, and ataxia in the blind-drunk mouse. *Proceedings of the National Academy of Sciences of the United States of America*, *104*(7), 2431–2436. https://doi.org/10.1073/pnas.0610222104

Jorquera, R. A., Huntwork-Rodriguez, S., Akbergenova, Y., Cho, R. W., & Troy Littleton, J. (2012). Complexin controls spontaneous and evoked neurotransmitter release by regulating the timing and properties of synaptotagmin activity. *Journal of Neuroscience*, *32*(50), 18234–18245. https://doi.org/10.1523/JNEUROSCI.3212-12.2012

Kaneda, R., Ueno, S., Yamashita, Y., Choi, Y. L., Koinuma, K., Takada, S., … Mano, H. (2005). Genome-wide screening for target regions of histone deacetylases in cardiomyocytes.

Circulation Research, *97*(3), 210–218. https://doi.org/10.1161/01.RES.0000176028.18423.07

Kimes, B. W., & Brandt, B. L. (1976). Properties of a clonal muscle cell line from rat heart. *Experimental Cell Research*, *98*(2), 367–381. https://doi.org/10.1016/0014-4827(76)90447-X

Kubicek, S., Gilbert, J. C., Fomina-yadlin, D., Gitlin, A. D., & Yuan, Y. (2012). Chromatin-targeting small molecules cause class-speci fi c transcriptional changes in pancreatic endocrine cells. *Proc Natl Acad Sci U S A*. https://doi.org/10.1073/pnas.1201079109/-/DCSupplemental.www.pnas.org/cgi/doi/10.1073/pnas.1201079109

Lorenz, M. A., El Azzouny, M. A., Kennedy, R. T., & Burant, C. F. (2013). Metabolome response to glucose in the β-cell line INS-1832/13. *Journal of Biological Chemistry*, *288*(15), 10923–10935. https://doi.org/10.1074/jbc.M112.414961

Louder, R. K., He, Y., López-Blanco, J. R., Fang, J., Chacón, P., & Nogales, E. (2016). Structure of promoter-bound TFIID and model of human pre-initiation complex assembly. *Nature*, *531*(7596), 604–609. https://doi.org/10.1038/nature17394

Malsam, J., & Söllner, T. H. (2011). Organization of SNAREs within the Golgi stack. *Cold Spring Harbor Perspectives in Biology*, *3*(10), 1–17. https://doi.org/10.1101/cshperspect.a005249

Mandon, B., Nielsen, S., Kishore, B. K., & Knepper, M. a. (1997). Expression of syntaxins in rat kidney. *The American Journal of Physiology*, *273*(5 Pt 2), F718–F730.

Maximov, A., Shin, O. H., Liu, X., & Südhof, T. C. (2007). Synaptotagmin-12, a synaptic vesicle phosphoprotein that modulates spontaneous neurotransmitter release. *Journal of Cell Biology*, *176*(1), 113–124. https://doi.org/10.1083/jcb.200607021

Menard, C., Pupier, S., Mornet, D., Kitzmann, M., Nargeot, J., & Lory, P. (1999). Modulation of L-type calcium channel expression during retinoic acid- induced differentiation of H9C2 cardiac cells. *Journal of Biological Chemistry*, *274*(0021-9258 SB-IM), 29063–29070. https://doi.org/10.1074/jbc.274.41.29063

Mill, J., Curran, S., Kent, L., Gould, A., Huckett, L., Richards, S., … Asherson, P. (2002). Association study of a SNAP-25 microsatellite and attention deficit hyperactivity disorder. *American Journal of Medical Genetics - Neuropsychiatric Genetics*, *114*(3), 269–271. https://doi.org/10.1002/ajmg.10253

Nagy, G., Milosevic, I., Fasshauer, D., Muller, E. M., de Groot, B. L., Lang, T., … Sorensen, J. B. (2005). Alternative splicing of SNAP-25 regulates secretion through nonconservative substitutions in the SNARE domain. *Mol Biol Cell*, *16*(12), 5675–5685. https://doi.org/E05-07-0595 [pii]\r10.1091/mbc.E05-07-0595

Nakayama, T., & Akagawa, K. (2017). Transcription regulation mechanism of the syntaxin 1A gene via protein kinase A. *Biochemical Journal*, *474*(14), 2465–2473. https://doi.org/10.1042/BCJ20170249

Nakayama, T., Mikoshiba, K., & Akagawa, K. (2016). The cell- and tissue-specific transcription mechanism of the TATA-less syntaxin 1A gene. *FASEB Journal*, *30*(2), 525–543. https://doi.org/10.1096/fj.15-275529

Parameswaran, S., Kumar, S., Verma, R. S., & Sharma, R. K. (2013). Cardiomyocyte culture — an update on the in vitro cardiovascular model and future challenges. *Canadian Journal of Physiology and Pharmacology*, *91*(12), 985–998. https://doi.org/10.1139/cjpp-2013-0161

Pereira, S. L., Ramalho-Santos, J., Branco, A. F., Sardão, V. A., Oliveira, P. J., & Carvalho, R. A. (2011). Metabolic remodeling during H9c2 myoblast differentiation: Relevance for in

vitro toxicity studies. *Cardiovascular Toxicology*, *11*(2), 180–190. https://doi.org/10.1007/s12012-011-9112-4

Peters, C. G., Miller, D. F., & Giovannucci, D. R. (2006). Identification, localization and interaction of SNARE proteins in atrial cardiac myocytes. *Journal of Molecular and Cellular Cardiology*, *40*(3), 361–374. https://doi.org/10.1016/j.yjmcc.2005.12.007

Rizo, J., & Rosenmund, C. (2008). Synaptic vesicle fusion. *Nature Structural & Molecular Biology*, *15*(n7), 665–674. https://doi.org/10.1038/nsmb.1450

Ruiz, M., Courilleau, D., Jullian, J. C., Fortin, D., Ventura-Clapier, R., Blondeau, J. P., & Garnier, A. (2012). A Cardiac-Specific Robotized Cellular Assay Identified Families of Human Ligands as Inducers of PGC-1α Expression and Mitochondrial Biogenesis. *PLoS ONE*, *7*(10). https://doi.org/10.1371/journal.pone.0046753

Ryabinin, A. E., Sato, T. N., Morris, P. J., Latchman, D. S., & Wilson, M. C. (1995). Immediate upstream promoter regions required for neurospecific expression of SNAP-25. *Journal of Molecular Neuroscience*, *6*(3), 201–210. https://doi.org/10.1007/BF02736765

Sagnella, G. A. (2002, June 1). The heart as an endocrine organ. *Biologist*. European Society of Endocrinology. https://doi.org/10.1097/AIA.0b013e31824d88a3

Saito, Y. (2010, November 1). Roles of atrial natriuretic peptide and its therapeutic use. *Journal of Cardiology*. Elsevier. https://doi.org/10.1016/j.jjcc.2010.08.001

Salunkhe, V. A., Ofori, J. K., Gandasi, N. R., Salö, S. A., Hansson, S., Andersson, M. E., … Eliasson, L. (2017). MiR-335 overexpression impairs insulin secretion through defective priming of insulin vesicles. *Physiological Reports*, *5*(21), e13493. https://doi.org/10.14814/phy2.13493

Shimada, M., Yanai, Y., Okazaki, T., Yamashita, Y., Sriraman, V., Wilson, M. C., & Richards, J.

S. (2007). Synaptosomal-associated protein 25 gene expression is hormonally regulated during ovulation and is involved in cytokine/chemokine exocytosis from granulosa cells. *Molecular Endocrinology (Baltimore, Md.)*, *21*(10), 2487–2502. https://doi.org/10.1210/me.2007-0042

Song, Y., Liu, L., Li, G., An, L., & Tian, L. (2017). Trichostatin A and 5-Aza-2′-Deoxycytidine influence the expression of cold-induced genes in Arabidopsis. *Plant Signaling and Behavior*, *12*(11). https://doi.org/10.1080/15592324.2017.1389828

Sriraman, V., Rudd, M. D., Lohmann, S. M., Mulders, S. M., & Richards, J. S. (2006). Cyclic Guanosine 5′-Monophosphate-Dependent Protein Kinase II Is Induced by Luteinizing Hormone and Progesterone Receptor-Dependent Mechanisms in Granulosa Cells and Cumulus Oocyte Complexes of Ovulating Follicles. *Molecular Endocrinology*, *20*(2), 348–361. https://doi.org/10.1210/me.2005-0317

Steg, P. G., James, S. K., Atar, D., Badano, L. P., Lundqvist, C. B., Borger, M. A., … Wallentin, L. (2012). ESC Guidelines for the management of acute myocardial infarction in patients presenting with ST-segment elevation. *European Heart Journal*, *33*(20), 2569–2619. https://doi.org/10.1093/eurheartj/ehs215

Sucharov, C. C., Langer, S., Bristow, M., & Leinwand, L. (2006). Shuttling of HDAC5 in H9C2 cells regulates YY1 function through CaMKIV/PKD and PP2A. *American Journal of Physiology. Cell Physiology*, *291*(5), C1029–C1037. https://doi.org/10.1152/ajpcell.00059.2006

Sudhof, T. C., & Rothman, J. E. (2009). Membrane Fusion: Grappling with SNARE and SM Proteins. *Science*, *323*(5913), 474–477. https://doi.org/10.1126/science.1161748

Thomas, L., Hartung, K., Langosch, D., Rehm, H., Bamberg, E., Franke, W. W., & Betz, H.

(1988). Identification of synaptophysin as a hexameric channel protein of the synaptic vesicle membrane. *Science*, *242*(4881), 1050–1053. https://doi.org/10.1126/science.2461586

Verderio, C., Pozzi, D., Pravettoni, E., Inverardi, F., Schenk, U., Coco, S., … Matteoli, M. (2004). SNAP-25 Modulation of Calcium Dynamics Underlies Differences in GABAergic and Glutamatergic Responsiveness to Depolarization. *Neuron*, *41*(4), 599–610. https://doi.org/10.1016/S0896-6273(04)00077-7

Waby, J. S., Bingle, C. D., & Corfe, B. M. (2008). Post-translational control of sp-family transcription factors. *Current Genomics*, *9*(5), 301–311. https://doi.org/10.2174/138920208785133244

Watkins, S. J., Borthwick, G. M., & Arthur, H. M. (2011). The H9C2 cell line and primary neonatal cardiomyocyte cells show similar hypertrophic responses in vitro. *In Vitro Cellular and Developmental Biology - Animal*, *47*(2), 125–131. https://doi.org/10.1007/s11626-010-9368-1

Whittle, N., & Singewald, N. (2014). HDAC inhibitors as cognitive enhancers in fear, anxiety and trauma therapy: Where do we stand? *Biochemical Society Transactions*, *42*(2), 569–581. https://doi.org/10.1042/BST20130233

Wood, M., Rymarchyk, S., Zheng, S., & Cen, Y. (2018). Trichostatin A inhibits deacetylation of histone H3 and p53 by SIRT6. *Archives of Biochemistry and Biophysics*, *638*, 8–17. https://doi.org/10.1016/j.abb.2017.12.009

Yoo, B. S., Lemaire, A., Mangmool, S., Wolf, M. J., Curcio, A., Mao, L., & Rockman, H. A. (2009). β 1 -Adrenergic receptors stimulate cardiac contractility and CaMKII activation in vivo and enhance cardiac dysfunction following myocardial infarction. *American Journal of*

Physiology - Heart and Circulatory Physiology, *297*(4), H1377–H1386. https://doi.org/10.1152/ajpheart.00504.2009

Yoshida, M., & Horinouchi, S. (1999). Trichostatin and leptomycin. Inhibition of histone deacetylation and signal-dependent nuclear export. *Annals of the New York Academy of Sciences*, *886*(1 ANTICANCER MO), 23–36. https://doi.org/10.1111/j.1749-6632.1999.tb09397.x

Zhang, C. L., McKinsey, T. A., Chang, S., Antos, C. L., Hill, J. A., & Olson, E. N. (2002). Class II histone deacetylases act as signal-responsive repressors of cardiac hypertrophy. *Cell*, *110*(4), 479–488. https://doi.org/10.1016/S0092-8674(02)00861-9

Zhang, J., Gao, Y., Yu, M., Wu, H., Ai, Z., Wu, Y., … Zhang, Y. (2015). Retinoic acid induces embryonic stem cell differentiation by altering both encoding RNA and microRNA expression. *PLoS ONE*, *10*(7), e0132566. https://doi.org/10.1371/journal.pone.0132566